European Journal of Pharmaceutics and Biopharmaceutics 183 (2023) 74–91

Contents lists available at ScienceDirect

European Journal of Pharmaceutics and Biopharmaceutics

journal homepage: www.elsevier.com/locate/ejpb

Research paper

Can amphotericin B and itraconazole be co-delivered orally? Tailoring oral fixed-dose combination coated granules for systemic mycoses

Raquel Fernández-García [a], David Walsh [b], Peter O'Connell [b], Karla Slowing [c], Rafaela Raposo [d], M. Paloma Ballesteros [a,e], Aurora Jiménez-Cebrián [f], Manuel J. Chamorro-Sancho [f], Francisco Bolás-Fernández [g], Anne Marie Healy [b], Dolores R. Serrano [a,e,*]

[a] Departamento de Farmacia Galénica y Tecnología Alimentaria, Facultad de Farmacia, Universidad Complutense de Madrid, Plaza de Ramón y Cajal, s/n, 28040 Madrid, Spain
[b] School of Pharmacy and Pharmaceutical Sciences, Trinity College Dublin, Dublin 2, Ireland
[c] Departamento de Farmacología, Farmacognosia y Botánica, Facultad de Farmacia, Universidad Complutense de Madrid, Plaza de Ramón y Cajal, s/n, 28040 Madrid, Spain
[d] Seccion Departamental de Fisiología, Facultad de Farmacia, Universidad Complutense de Madrid, Plaza Ramón y Cajal s/n, 28040 Madrid, Spain
[e] Instituto Universitario de Farmacia Industrial, Facultad de Farmacia, Universidad Complutense de Madrid, Plaza de Ramón y Cajal, s/n, 28040 Madrid, Spain
[f] Centro Militar Canino de la Defensa, Avenida Carabanchel Alto, 17, 28044 Madrid, Spain
[g] Departamento de Microbiología y Parasitología, Facultad de Farmacia, Universidad Complutense de Madrid, Plaza de Ramón y Cajal, s/n, 28040 Madrid, Spain

ARTICLE INFO

Keywords:
Oral delivery
Amphotericin B
Fixed-dose combination
Granules
Spray-coating
Itraconazole
Quality by design
Antifungal therapy
Azoles
Candida spp

ABSTRACT

The incidence and prevalence of invasive fungal infections have increased significantly over the last few years, leading to a global health problem due to the lack of effective treatments. Amphotericin B (AmB) and itraconazole (ITR) are two antifungal drugs with different mechanisms of action. In this work, AmB and ITR have been formulated within granules to elicit an enhanced pharmacological effect, while enhancing the oral bioavailability of AmB. A Quality by Design (QbD) approach was utilised to prepare fixed-dose combination (FDC) granules consisting of a core containing AmB with functional excipients, such as inulin, microcrystalline cellulose (MCC), chitosan, sodium deoxycholate (NaDC) and Soluplus® and polyvinyl pyrrolidone (PVP), coated with a polymeric layer containing ITR with Soluplus® or a combination of Poloxamer 188 and hydroxypropyl methyl cellulose-acetyl succinate (HPMCAS). A Taguchi design of experiments (DoE) with 7 factors and 2 levels was carried out to understand the key factors impacting on the physicochemical properties of the formulation followed by a Box-Behnken design with 3 factors in 3 levels chosen to optimise the formulation parameters. The core of the FDC granules was obtained by wet granulation and later coated using a fluidized bed. *In vitro* antifungal efficacy was demonstrated by measuring the inhibition halo against different species of *Candida* spp., including *C. albicans* (24.19–30.48 mm), *C. parapsilosis* (26.38–27.84 mm) and *C. krusei* (11.48–17.92 mm). AmB release was prolonged from 3 to 24 h when the AmB granules were coated. *In vivo* in CD-1 male mice studies showed that these granules were more selective towards liver, spleen and lung compared to kidney (up to 5-fold more selective in liver, with an accumulation of 8.07 μg AmB/g liver after twice-daily 5 days administration of granules coated with soluplus-ITR), resulting in an excellent oral administration option in the treatment of invasive mycosis. Nevertheless, some biochemical alterations were found, including a decrease in blood urea nitrogen (~17 g/dl) and alanine aminotransferase (<30 U/l) and an increase in the levels of bilirubin (~0.2 mg/dl) and alkaline phosphatase (<80 U/l), which could be indicative of a liver failure. Once-daily regimen for 10 days can be a promising therapy.

* Corresponding author at: Departamento de Farmacia Galénica y Tecnología Alimentaria, Facultad de Farmacia, Universidad Complutense de Madrid, Plaza de Ramón y Cajal, s/n, 28040 Madrid, Spain.
E-mail address: drserran@ucm.es (D.R. Serrano).

https://doi.org/10.1016/j.ejpb.2023.01.003
Received 24 September 2022; Received in revised form 6 December 2022; Accepted 3 January 2023
Available online 7 January 2023

1. Introduction

The incidence and prevalence of invasive fungal infections, mostly caused by *Candida* spp., have increased progressively over the last decade. This has resulted in a global health problem, which has been worsened in immunocompromised and critically ill patients [1–3]. Apart from that, the emergence of resistance hinders the use of antimicrobials as their effectiveness has been dramatically reduced [4,5]. To address this situation, the manufacturing of fixed-dose combination (FDC) products is a flourishing and promising approach based on the combination of drugs with different mechanisms of action triggering a synergistic effect and curbing the appearance of resistances. In addition, there are other multiple advantages associated with fixed-dose combination (FDC) therapies, such as i) the reduction of adverse effects as a lower dose is necessary to achieve the same efficacy as monotherapy, ii) a higher efficacy and iii) an improvement in therapeutic compliance by patients since treatment duration and polypharmacy is reduced [6–8]. In the treatment of infective diseases, FDC therapy has been frequently utilised in patients infected with the human immunodeficiency virus (HIV), which requires at least two different antivirals to avoid resistance. FDCs have also been developed to treat other disorders such as metabolic disorders, including diabetes, dyslipidemia, and hypertension [9–11].

Regarding combined antifungal therapy, results obtained so far are also promising. The combination of parenterally administered amphotericin B (AmB) with azoles (i.e., posaconazole, itraconazole, fluconazole) is especially useful in critically ill patients for whom the administration of high doses of AmB is contraindicated due to the high risk of adverse effects, including renal failure, dyspnoea, hypokalaemia, nausea, vomiting and infusion-related chills when using Fungizone® [12,13]. Although the risk of nephrotoxicity has been diminished since liposomal AmB (AmBisome®) has been implemented in clinic, patients might still experience with the other adverse effects such as anemia [14,15]. The risk of haemolysis is higher when formulations are parenterally administered; however, the oral administration can ameliorate the symptomatology. The combination of both drugs allows the administration of lower AmB doses, reducing its adverse effects and at the same time, achieving a synergistic effect with azoles [16–18]. Currently, AmB is only commercialised as parenteral formulations for intravenous administration due to its poor solubility and permeability in an aqueous medium (with an oral bioavailability of ~ 0.2–0.9 %) [19,20]. The lack of an orally bioavailable AmB formulation is a handicap, especially in developing countries where access to hospitals may be hampered and intravenous AmB can lead to anaphylactic reactions and severe infusion-related adverse effects [20]. AmB can be found in three different aggregation states, which can be easily identified by UV–vis spectrometry. The monomeric AmB state can be identified at 406–490 nm, while the characteristic dimer (also known as oligomer) peak is found between 328 and 3490 nm. A poly-aggregated AmB can also be identified by UV–vis, although the peaks show a lower intensity as for the other states located between 406 and 420 nm, 383–385 nm and 360–363 nm. Identifying which aggregation state is predominant in AmB formulations is key, as the monomeric state has been found to be the one with the highest toxicity. This means that the ratio between the dimeric and the monomeric peak greater than 1 is related with lower toxicity.

To date, combined antifungal therapy is based on the administration of different drugs separately, in some cases through different administration routes, which makes the regime more complicated and reduces patient compliance and adherence [8]. The manufacturing of antifungal FDC products is challenging as most drugs are poorly water-soluble with different pharmacokinetic profiles. Physicochemical incompatibilities between drugs may result in a decrease in bioavailability [21]. However, the development of an oral FDC product for the treatment of systemic mycoses is an unmet clinical need. AmB possesses antifungal activity due to a dual mechanism of action causing oxidative stress in the cell but also binding to the ergosterol in plasma membranes, creating a pore that allows the leakage of ions from the cytoplasm of fungal cells, leading to apoptosis [22–24]. Formulating AmB with other azoles such as itraconazole (ITR) as a FDC product could be an interesting approach to enhance the overall antifungal efficacy. ITR was selected as a model antifungal drug, as it can block ergosterol synthesis through a different mechanism of action by inhibiting the lanosterol 14α-demethylase enzyme. This drug is characterised also by low aqueous solubility and a poor dissolution rate [25]. However, unlike AmB, ITR is currently available as hydroxypropyl-β-cyclodextrin-based suspensions and capsules containing coated pellets for oral administration and has demonstrated a very low toxicity [26,27]. Nevertheless, ITR could cause some mild adverse effects, including fluid retention, gastrointestinal intolerance and headache [28]. Abnormalities in liver function are rare such as higher levels of bilirubin and serum alkaline phosphatase [29].

Wet granulation has been traditionally utilised in pharmaceutical development to obtain micron-sized granules to improve the physicochemical properties of the powder mixture such as flow and compactability before tableting. Granules can be also used a final dosage form stored in sachets to enhance oral drug bioavailability. For this purpose, it is crucial to find an optimal balance between the drug and the excipients selected. Microcrystalline cellulose (MCC) is widely utilised in the manufacturing of granules as a diluent as promotes a rapid wetting of the powder mixture, but also it provides granule strength reducing their brittleness during spray-coating [30]. Binding agents are crucial to make the granulation process successful for which polyvinyl pyrrolidone (PVP), a synthetic polymer, was chosen [31]. Disintegrants are also key to ensure the granules can release the drug in a faster manner upon contact with physiological fluids. Chitosan is a natural polymer, selected as disintegrant for the manufacturing of the granules as also possesses bioadhesive properties allowing a better penetration through the intestinal mucus enhancing drug absorption [32]. The utilisation of surfactants or solubilisers is key to enhance the solubility of poorly soluble drugs, such as AmB or ITR. In this work, Soluplus®, a synthetic polymer with excellent solubilising properties, and sodium deoxycholate (NaDC) traditionally used for conventional parenteral AmB formulations, were selected to be included in the granule formulation [33]. Additionally, inulin, a polysaccharide with prebiotic properties, was assessed as a filler-binder in wet granulation [34,35]. AmB can cause gastrointestinal toxicity and hence, the addition of prebiotics could alleviate these symptoms.

The design of an optimal granule formulation with two poorly water soluble drugs is challenging and hence, quality by design (QbD) tools have arisen for implementation in pharmaceutical research and development in the last decades, for both lab and industrial scale, with the aim of ensuring a high quality of the final dosage form, minimising waste and making the optimization process cost-time-effective [36]. For this purpose, different steps usually take place, including a pre-screening design (e.g. Taguchi or Plackett-Burman) in order to identify the critical factors of the process. When the most influential factors have been identified, more robust models (e.g. Box-Behnken), known as response surface models, are employed to find the optimal design space [36,37].

The hypothesis underpinning this work is that the combination of AmB with ITR in an oral dosage form may lead to a more effective and safer antifungal treatment than monotherapy, avoiding parenteral-route-related side effects. The combination of different mechanisms of action may result in an additive effect and thus, a lower dose would be required to elicit the same pharmacological effect through different mechanisms of biodistribution. The main objective of this work was the engineering and optimisation (applying a Quality by Design, QbD approach) of innovative oral controlled release FDC formulations containing an AmB core with an ITR coated layer to be administered as water-dispersible granules stored in sachets. Active excipients were employed to enhance the oral bioavailability of both drugs, but also to minimise the adverse effects along the gastrointestinal tract such as inulin. AmB was incorporated in the core of the granule to protect it

from the acid gastrointestinal pH while ITR was incorporated in the coating layer mimicking the conventional formulation Sporanox® to enhance its surface area and dissolution. The physicochemical performance of the FDC formulation was evaluated. Oral pharmacokinetic and toxicological studies were performed to assess its *in vivo* profile.

2. Materials and methods

2.1. Materials

AmB was purchased from North China Pharmaceutical Huasheng Co (Hebei, China). ITR was purchased from Kemprotec Ltd. (Camforth, United Kingdom). Inulin Frutafit® HD with an average degree of polymerization of 10 was a gift from Sensus (Roosendaal, The Netherlands). MCC Avicel® PH-101 was supplied from FMC Corporation (Pennsylvania, USA). Low-viscosity chitosan was purchased from Guinama S.L.U. (Valencia, Spain). Sodium deoxycholate (NaDC), ethanol, and dichloromethane (DCM) were supplied from Sigma-Aldrich Chemie GmbH (Buchs, Switzerland). Polyvinyl caprolactam-polyvinyl acetate-polyethylene glycol graft co-polymer (Soluplus®) and PVP Kollidon® 17PF and 90F (K17 and K90, respectively) were a gift from BASF SE (Ludwigshafen, Germany). Sodium salts (Na_2HPO_4 and NaH_2PO_4) were purchased from Panreac Química S.A.U. (Barcelona, Spain), while polypropylene glycol-polyethylene glycol co-polymer Poloxamer 188 (Pluronic® F68) was purchased from Thermo Fisher Scientific Inc. (Massachusetts, USA), and hydroxypropyl methylcellulose-acetate succinate (HPMCAS) Aqoat® AS-HG was a sample gift kindly provided by Shin-Etsu Chemical Co. Ltd. (Tokyo, Japan).

2.2. Methods

2.2.1. Preparation of FDC coated granules

FDC granules were obtained by wet granulation followed by spray-coating. The granules consisted of AmB, inulin, MCC, chitosan, NaDC, Soluplus®, and phosphate salts which were weighed and mixed using a mortar and pestle. For optimisation purposes, two types of AmB-surfactant complex were manufactured; the first one consisted of a physical mixture of the two components and the other complex was obtained by freeze-drying (Methods S1 supplementary material). 2.5 % aqueous solution of PVP was added to the mixture drop by drop as a binder until a solid wet mass was obtained. The mixture was mesh strained at consecutive sieve openings (1 mm, 710 μm, 500 μm, 350 μm, and 149 μm) and was dried at room temperature overnight. The granules collected in each fraction were separated and weighed.

The larger mass fraction (fractions collected on the 710 and 500 μm sieves) was selected to avoid attrition during the spray coating and was placed inside a Mini-Glatt® fluidised bed coater equipped with a Wurster insert (Glatt®, Binzen, Germany). Different solutions were used to spray layer the AmB granules, with a 1:2 ITR: excipient weight ratio in solution. The excipients used in the coating layer were: Soluplus® or a mixture of HPMCAS and Poloxamer 188 (2:1 w:w ratio) which were dissolved in 170 ml of a mixture of ethanol and DCM (1:1 v:v) with a drug concentration of 8.4 mg/ml. The process parameters were as follows: 40 °C inlet temperature, 0.5 mm nozzle diameter, 3.8 g/min spray rate, 25 m^3/h nitrogen flow rate, and 0.8 bar atomisation pressure.

2.2.2. Optimisation of AmB cores obtained by wet granulation

Optimisation took place in two steps by QbD, utilising Design-Expert® software version 10 (Stat-Ease®, Minneapolis, USA). A seven-factor eight-run Taguchi design (2^7) was employed as a pre-screening step to identify the formulation and process parameters that could influence the quality of the product. Once the critical quality attributes (CQAs) were identified, a three-factor three-level Box-Behnken design (3^3) with 17 runs was performed to optimise the final formulation.

In the pre-screening Taguchi design, four factors were numerical and three were categorical. The categorical independent variables were: i) the type of binder (PVPK17 or PVPK90), ii) the type of surfactant (NaDC or Soluplus®) and iii) the type of AmB-surfactant complex (physical mixture or freeze-dried, as previously described [38]). The numerical factors were: i) the amount of MCC (5 and 25 %), ii) the amount of chitosan (1 and 10 %), iii) the amount of AmB (5 and 25 %) and iv) the volume of 2.5 % PVP solution added for a 2 g batch (4 and 8 ml). Inulin was added to the mixture up to a final amount of 2 g per batch.

The selected dependent variables were: amount dissolved at 60 min, yield, core size ratio (expressed as the ratio between mass fraction > 500 μm/ mass fraction collected < 500 μm), antifungal activity against *Candida albicans* (expressed as the diameter of inhibition halo) and AmB aggregation state (expressed as the ratio dimer/monomer, as previously described [39]). Dependent variables were investigated as described below.

The amount of AmB dissolved after 60 min was tested in simulated intestinal fluid (SIF) without enzymes (pH 6.8), which was prepared by dissolving KH_2PO_4 and NaCl in deionised water [39]. For this purpose, an Erweka DT80 dissolution tester apparatus (Erweka GmbH, Hessen, Germany) was utilised. The absorbance of each sample was measured at 328 and 406 nm using a PharmaSpec® UV–visible spectrophotometer (Shimadzu, Kyoto, Japan). The absorbance measurement was utilised to calculate the aggregation state ratio. The ratio dimer/monomer was calculated by dividing the absorbance at 328 nm (characteristic of the dimeric form of AmB) and absorbance at 406 nm (characteristic of monomeric AmB) [22,24].

AmB granules were collected, separated, and weighed after overnight drying (at room temperature) to calculate core size ratio and yield. These parameters were obtained as follows (Eq. (1) and (2)):

$$Core\ size\ ratio = \frac{A}{B} \tag{1}$$

$$Yield\ (\%) = \frac{A+B}{C} \times 100 \tag{2}$$

where A was the weight of AmB cores larger than 500 μm after overnight drying, B was the weight of granules with a core size below 500 μm and C was the total weight of starting materials (theoretical weight).

In vitro activity against *C. albicans* was determined by agar diffusion assay, according to the European Pharmacopoeia standards as previously described [39,40].

After identifying the critical material attributes (CMAs), a three factor-three level Box-Behnken design was carried out. The selected factors for optimisation were the amount of MCC (5, 12.5 and 20 %), the ratio between AmB and surfactant (2:1, 1:1 and 1:2, w:w) and the ratio between NaDC and Soluplus® (2:1, 1:1 and 1:2 w:w). The other parameters tested during the Taguchi design were kept constant through all run formulations. All the same responses were analysed except for the *in vitro* antifungal activity.

DesignExpert® was used to calculate the Bonferroni and *t*-value limits in the Taguchi design and construct a multiple linear regression (MLR) model to find mathematical relationship among the responses, while analysis of variance (ANOVA) was performed to understand the significance of the different factors on the evaluated responses. Predicted values of all dependant variables for all runs were generated by substituting values of the numerical factors. The numerical optimisation method was used to choose the optimal formulation from the Box-Behnken design. The highest amount dissolved after 60 min and the highest yield were the chosen criteria for optimisation of the AmB core granules. The optimised formulation was subsequently coated with a single coating layer containing ITR (see Table 2 for composition). Three final formulations were obtained and further characterised.

2.2.3. Physicochemical characterisation of FDC coated granules

2.2.3.1. Drug content. Drug content was calculated by adding 2 ml of

Table 1
APS time points and conditions of coated granules.

Time (days)	Temperature (°C)	RH (%)
1	60	75
	70	10
		50
2	60	75
3	50	50
	70	10
		50
5	60	75
7	50	10
		50
	60	75
	70	10
		50
10	70	10
		50
14	50	10
		50
21	50	10

Table 2
Composition of the three optimised AmB formulations. AmB was located in the core for all formulations. Soluplus®, Poloxamer 188, and HMPCAS were utilised as binding agents. Key: ITR, itraconazole.

Formulation	Type of coating	Binding agents	Drug in the coating layer
F1	No coating	–	–
F2	Single layer	Soluplus®	ITR
F3	Single layer	HPMCAS Poloxamer 188	ITR

dimethylsulfoxide (DMSO) (Scharlab S.L., Barcelona, Spain) to 10 mg of granules (n = 3). The dispersion was then filtered through 0.45 μm PTFE filters (Thermo Fisher Scientific Inc., Massachusetts, USA) and diluted to be further analysed by HPLC. Samples were analysed using a Jasco HPLC (Jasco Co., Tokyo, Japan) with a DG-2080–53 3-line degasser, a LG-2080–02 ternary gradient unit, a PU-1580 intelligent HPLC pump, a UV-1575 intelligent UV/vis detector, and an AS-2050 Plus intelligent autosampler. The mobile phase consisted of 52:4.3:43.7 (v:v:v) acetonitrile: acetic acid: water for both drugs [41]. The mobile phase was filtered through a 0.45 μm Supor®-450 membrane filter with a diameter of 47 mm (Pall Co., Michigan, USA). Separation was carried out using a BDS Hypersil C18, 5 μm (200 × 4.6 mm) column (Thermo Fisher Scientific Inc., Massachusetts, USA) at a UV detection wavelength of 406 and 260 nm for AmB and ITR, respectively, with an injection volume of 100 μl. Elution took place using an isocratic method at room temperature with a flow rate of 1 ml/min. Peak evaluation was performed using Borwin software [41]. The linearity ($R^2 > 0.999$) for AmB was found between 0.1 and 20 μg/ml with a limit of quantification of 0.25 μg/ml while the linearity ($R^2 > 0.998$) for ITR was found between 0.2 and 50 μg/ml with a limit of quantification of 0.5 μg/ml.

2.2.3.2. Particle size distribution (PSD). PSD was measured by laser diffraction using a Mastersizer 2000 (Malvern Panalytical Ltd., Malvern, United Kingdom) (n = 3). A Scirocco dry powder feeder was utilised with 1 bar pressure and vibration feed rate of 50 %. The thickness of the coating layers was calculated by taking into account the median particle size (D_{50}) of the core and the coated formulation according to Eq. (3) [42]:

$$Thickness\ (nm) = \frac{D_{50}\ after\ coating - D_{50}\ before\ coating}{2} \quad (3)$$

2.2.3.3. Scanning electron microscopy (SEM). Morphology of the formulations was evaluated by SEM using a JSM 6335F (Jeol Ltd., Tokyo, Japan) equipped with a secondary electron detector, which provided an image resolution of 1.5 nm (at 15 kV) and 5 nm (at 1 kV). Pellets were previously cut in halves using a sharp blade to visualise the surface, the coating layer, and the core of the coated formulation. Samples were placed onto carbon tabs, mounted on aluminum pins and sputtered with gold.

2.2.3.4. Modulated temperature differential scanning calorimetry (MT-DSC). MT-DSC analysis was performed using a DSC Q200 (TA Instruments®, Delaware, USA) with nitrogen as the purge gas. Samples (2–3 mg) were placed in aluminum pans and scanned over a temperature range of 0–200 °C with a modulation rate of 0.8 °C every 60 s and a scanning rate of 5 °C/min [39]. Data were processed using TA Universal Analysis® software version 4.5A (TA Instruments®, Delaware, USA). Calibration of the instrument was carried out using indium as standard. Temperatures of melting events (n = 3) refer to onset temperature.

2.2.3.5. Thermogravimetric analysis (TGA). Water content (n = 3) was quantified by TGA which was carried out using a TGA Q50 measuring module (TA Instruments®, Delaware, USA). Aluminum pans were utilised to perform the analysis and nitrogen was used as the purge gas. Samples were undertaken to a range of temperatures between 50 and 300 °C at a rate of 10 °C/min. Data were analysed using TA Universal Analysis® software version 4.5A (TA Instruments®, Delaware, USA).

2.2.3.6. Fourier-transform infrared spectroscopy (FTIR). FTIR spectra were acquired using a Spectrum 1 FT-IR spectrometer (PerkinElmer Inc., Massachusetts, USA) equipped with a UATR and ZnSc crystal accessory. Spectra (n = 6) were scanned in the range of 600–4000 cm^{-1}. Data interpretation was performed by using Spectragryph® software version 1.2.9 (The Spectroscopy Ninja®, Berchtesgaden, Germany).

2.2.3.7. Powder X-ray diffraction (PXRD). PXRD analysis was carried out utilising a Miniflex II diffractometer (Rigaku Co., Tokyo, Japan) with Ni-filtered Cu Kα radiation (1.54 Å) in triplicate. The tube voltage and tube current used were 30 kV and 15 mA, respectively. The PXRD patterns were recorded for 2θ ranging from 5° to 40° at a step scan rate of 0.05° per second.

2.2.3.8. Surface area. Surface area measurement based on the BET (Braunauer-Emmett-Teller) isotherm method was performed using a Micromeritics Gemini 2385c surface area and pore size analyser (Micromeritics Instrument Corp., Georgia, USA). The surface area for each sample was determined by nitrogen adsorption and BET multiple-point method, obtaining 6 points in the relative pressure range (P/P_0) of 0.05 and 0.3. Samples were previously prepared by purging under nitrogen overnight at 25 °C. Each average result was calculated on the basis of three measurements [43].

2.2.3.9. Dynamic vapour sorption (DVS). Vapour sorption experiments were performed using a DVS Advantage-1 automated gravimetric sorption analyser (Surface Measurement Systems Ltd., London, United Kingdom) at a temperature of 25 ± 0.1 °C. Water was selected as the probe vapour. An amount of 15–20 mg of sample was placed on the sample basket and dried at 0 % relative humidity (RH) for 1 h and then submitted to step changes of RH, from 10 to 90 %, and the opposite for desorption. The sample mass was allowed to reach equilibrium, defined as $dm/dt \leq 0.002$ mg/min over 10 min, before the RH was changed. Two sorption and desorption cycles were recorded [44] for each sample. Samples were evaluated by PXRD after DVS analyses.

2.2.4. Dissolution studies

Simulated gastric fluid (SGF, 500 ml) without enzymes was prepared using HCl and deionised water, adjusting the pH to 1.2. This medium was placed in an Erweka DT80 dissolution apparatus (Erweka GmbH, Hessen, Germany) and allowed to heat up to 37 °C for 1 h to simulate

physiological temperature. Then, 25 mg of granules were weighed and added to each vessel. Dissolution studies were performed using paddles at a rotation speed of 100 rpm and under sink conditions in two steps. First, SGF was utilised for the first 30 min; then, 400 ml of SIF supplemented with 0.5 % sodium dodecyl sulfate (Themo Fisher Scientific, Massachusetts, USA) to allow AmB dissolution in sink conditions was added to vessels. After the addition of SIF, the pH was adjusted up to 6.8 by adding 2.5 ml of a NaOH 30 % aqueous solution. All dissolution media were prepared according to Pharmacopoeia standards [45]. Samples (5 ml) were taken without replacement at several time points (5, 10, 15, 30, 45, 60, 90, 120, 150, 180, 240, 360, 480 and 1440 min). Samples were then centrifuged at 5000 rpm for 5 min and the supernatant was transferred to HPLC vials. Samples were analysed using the above-described HPLC methods. Dissolution studies were carried out in triplicate. The dissolution profile was fitted to different release kinetics models, including zero order (constant dissolution regardless of concentration, following a linear model), first order (release depends on the concentration), Higuchi (usually applied to drug release from an insoluble matrix as a square root of time-dependent process based on a Fickian diffusion), Korsmeyer-Peppas (drug release occurs from a polymeric system involving different release mechanisms simultaneously, such as diffusion of water into the polymeric matrix, swelling of the matrix and dissolution of the matrix and Hixson-Crowell (commonly used in formulations with uniform particle size, as dissolution depends on based on the cube root of the weight of the product) [43,46,47].

2.2.5. Accelerated predictive stability studies (APS)

All the formulations were kept refrigerated (4 ± 1.21 °C) in a desiccator containing silica gel (RH = 11.01 ± 1.64 % RH) before commencing the accelerated stability testing of the coated granules. The Cuspor Ageing System ™ was used to age each formulation. The relevant humidity capsules were placed into the Cuspor chambers which were put inside the oven at the selected temperature to ensure that equilibrium RH was reached before the aging of the formulations [42]. Samples (~5 mg) were weighed and placed in uncapped HPLC vials and introduced into the stability chambers, so being exposed to different conditions of temperature and RH (50 °C/10 % RH, 50 °C/50 % RH, 60 °C/75 % RH, 70 °C/10 % RH, and 70 °C/50 % RH) (Table 1). At different time points, samples were collected, dissolved in DMSO, further diluted with mobile phase, and analysed by the HPLC method detailed above.

Stability modelling was performed by fitting the AmB degradation kinetics to different models: including zero-order, first order, second order, Avrami, and diffusion. A humidity-corrected Arrhenius equation was used to understand the effect of temperature and RH on degradation (Eq. (4)) [48]:

$$\ln K = \ln A - \frac{E_a}{RT} + B(RH) \tag{4}$$

where K is the degradation constant, A is the collision frequency, E_a is the activation energy, R is the gas constant, T is the absolute temperature, B is the humidity sensitivity factor and RH is the relative humidity. The B term was calculated using the following equation (Eq. (5)):

$$\frac{\mathrm{Ln}\left(\frac{k_1}{k_2}\right)}{RH_1 - RH_2} \tag{5}$$

where k_1 and k_2 are the degradation constants calculated at the same temperature but different relative humidity, RH_1 and RH_2, respectively. An averaged B term calculated at the different temperatures was used. Long-term stability studies were performed at 25 °C/10 % RH and 4 °C/10 % RH.

2.2.6. In vitro antifungal activity

FDC coated granules were tested against three species of *Candida* spp., *C. albicans, C. parapsilosis,* and *C. krusei.* The assay was performed according to the European Pharmacopoeia [49]. Before the experiment, yeasts were isolated in a Petri dish containing Sabouraud dextrose agar (Becton, Dickinson and Co., New Jersey, USA) and incubated at 30 °C for 72 h. Once isolated, Müller-Hinton agar (Laboratorios Conda S.A., Madrid, Spain), supplemented with glucose (Panreac Química S.A.U., Barcelona, Spain) (2 % w/v) was prepared and autoclaved at 121 °C for 20 min. The experiment was performed in aseptic conditions. Methylene blue (0.5 mg/ml) was added to sterile Müller-Hinton agar for contrast purposes. One isolated yeast colony was dispersed in sterile NaCl 0.9 % (Laboratorios ERN, S.A., Barcelona, Spain) and later adjusted to 0.1 Abs at 600 nm wavelength, according to the McFarland factor. The yeast suspension was inoculated in sterile Müller-Hinton agar at 40 °C and the mixture was poured onto Petri dishes. Later, 6 mm paper disks embedded with 20 μl of an aqueous suspension containing the granules (with an AmB concentration of 0.5/ml) were placed onto the inoculated agar, once it solidified. The formulations were compared to standards of AmB and ITR dissolved in DMSO and AmB Neosensitabs™ (commercial disks containing 10 μg of AmB) (Rosco Diagnostica S/A, Taastrup, Denmark). All formulations and standards were adjusted to 10 μg of AmB. The inhibition halos were measured after incubation at 30 °C for 48 h. Each formulation was tested in quadruplicate.

2.2.7. Ex vivo red blood cells (RBC) haemolysis assay

Haemolytic toxicity was studied by a previously described method with some modifications [50,51]. Blood was taken from a healthy human donor and placed into lithium-heparin-coated Vacutainer™ tubes (Becton, Dickinson and Co., New Jersey, USA) to avoid coagulation. Tubes were centrifuged at 1000 g for 5 min to precipitate RBC, while plasma (supernatant) was removed. RBC were washed with a 150 mM NaCl solution and centrifugation was repeated several times. Later, phosphate buffer (pH 7.4) was added to RBC up to a concentration of 4 %.

Diluted RBC and granules dispersed in water at different concentrations (ranging from 0.78 to 100 μg/ml) were placed in 96-well plates in a 1:1 v:v ratio. All samples were tested in triplicate. 20 % Triton® X-100 (Merck KGaA, Darmstadt, Germany) and PBS (pH 7.4) were used as positive and negative control wells, respectively. Afterwards, the plates were incubated at 37 °C for 1 h using an orbital rocker. Plates were then centrifuged at 500 g for 5 min to precipitate intact RBC and the supernatant was transferred to a new clear plate to measure the absorbance at 570 nm using a BioTek ELx808 UV-plate reader (BioTek Instruments Inc, Vermont, USA) to determine the amount of haemoglobin released, indicating cell lysis.

Haemolytic toxicity was calculated by using the following equation (Eq. (6)):

$$Haemolysis\,(\%) = \frac{ABS(sample) - ABS(PBS)}{ABS(Triton\,X)} \times 100 \tag{6}$$

Data was analysed using Compusyn™ v1.0 software (Combosyn Inc., New Jersey, USA) and toxicity was expressed in HC_{50} (concentration needed to produce haemolysis in 50 % of RBCs).

2.2.8. Oral pharmacokinetic studies (PK)

All experiments were carried out in male CD-1 mice (6-week-old) in the animal house at the School of Medicine at Universidad Complutense de Madrid. All experiments were performed according to the Ethical Committee approved by the Community of Madrid (PROEX 151/19). Animals were randomly allocated into four groups and were allowed free access to water up to the day before single-dose administration. In total, two test formulations (F1 and F2) and two control formulations were evaluated. The control formulations consisted of AmB dispersed in deionised water and a 10 mg/ml oral suspension containing ITR (Sporanox®; Janssen Global Services LLC, Beerse, Belgium). Samples containing AmB were dispersed with deionised water giving a 1 mg/mL AmB concentration and then administered by oral gavage at a 5 mg/kg dose, while Sporanox® was administered at a 3.25 mg/kg dose of ITR.

The dose of Sporanox® was calculated based on the drug loading contained in F2 for ITR (See Table 2). Each formulation was administered to 24 mice which were split into 6 groups (n = 4) and euthanised using a CO_2 chamber at different time points (0.5, 1, 2, 4, 6, and 24 h). An oral multidose experiment was also carried out with the same four formulations at the same doses as described above (5 mg/kg and 3.25 mg/kg of AmB and ITR). Formulations were orally administered either once or twice daily for five days. Animals had free access to food and water during the whole experiment. Animals were then euthanised 24 h following the completion of once-daily treatment and 12 h following the completion of twice-daily treatment.

Once euthanised, blood was taken directly from the heart and placed in heparin/lithium Vacutainer™ tubes. Plasma was separated by centrifugation (1000 g, 5 min) and kept in the freezer (-40 °C) until analyses were performed. Drug extraction was carried out by mixing 100 µl of plasma with 100 µl of methanol. Samples were spiked with 10 µl of a 100 µg/ml stock solution of meloxicam used as an internal standard (Merck KGaA, Darmstadt, Germany). The mixture was then vortexed and left overnight at −40 °C to precipitate plasma proteins. After that, samples were centrifuged (16000 g, 10 min) and the supernatant was transferred to HPLC vials. HPLC analysis was performed as described above.

Tissue sample preparation (liver, kidney, spleen, and lung) was performed by adding PBS pH 7.4 at a concentration of 0.5, 0.25, 0.1, and 0.1 g of tissue/ml of solution, respectively. After tissue homogenisation, 10 µl of meloxicam (100 µg/ml) was added. Drugs were extracted by adding methanol in a 1:2 ratio of tissue homogenate: methanol. Samples were vortexed for 5 min and left at −40 °C overnight. Afterwards, samples were centrifuged (16000 g, 10 min) and the supernatant was analysed by the previously described HPLC method.

Urine and bile samples were directly extracted from the bladder and gallbladder, respectively. Samples (10 µl) were collected and methanol (90 µl) was added. Samples were vortexed and then centrifuged (16000 g, 10 min) and the supernatant was analysed by HPLC.

Non-compartmental pharmacokinetic data analysis was carried out using PKSolver [52]. The area under the plasma concentration versus time curve (AUC) and the area under the first moment curve (AUMC) from 0 to 24 h were calculated according to the linear trapezoidal method. The terminal phase elimination rate constant (λ) was calculated from the negative slope of the natural log (Ln)-terminal portion of the plasma concentration versus the time curve. λ was utilized to calculate the terminal elimination half-life ($t_{1/2}$) (Eq. (7)):

$$t_{1/2} = \frac{0.693}{\lambda} \tag{7}$$

The AUC and AUMC were extrapolated from the last time point to infinitive (Eq. (8) and (9)), where C_{24h} is the plasma concentration at 24 h:

$$AUC = \frac{C_{24h}}{\lambda} \tag{8}$$

$$AUMC = \frac{C_{24h} \times 24}{\lambda} + \frac{C_{24h}}{\lambda^2} \tag{9}$$

Total body clearance (Cl), volume of distribution (Vd) and mean residence time (MRT) were also calculated (Eq. (10)–(12)):

$$Cl = \frac{Dose}{AUC_{0\to\infty}} \tag{10}$$

$$Vd = \frac{Dose}{\lambda \times AUC_{0\to\infty}} \tag{11}$$

$$MRT = \frac{AUMC_{0\to\infty}}{AUC_{0\to\infty}} \tag{12}$$

2.2.9. In vivo toxicological analysis

Toxicological analyses were carried out in plasma samples extracted from animals from the twice-daily oral PK multiple-dose study. For this purpose, a VetScan® VS2 chemistry analyser (Zoetis Inc., New Jersey, USA) was utilised. Different blood parameters were measured, including albumin, alkaline phosphatase, alanine aminotransferase, amylase, bilirubin, blood urea nitrogen, total calcium, inorganic phosphorus, creatinine, glucose, ions (Na^+ and K^+), total protein and globulin.

2.2.10. Statistical analysis

Minitab® 16 (Minitab Inc, Coventry, United Kingdom) was utilised to perform one-way ANOVA. Tukey's test was used to establish a comparison among formulations and find statistically significant differences between groups.

3. Results

3.1. Preparation of FDC-coated granules

Three formulations were engineered and their composition is shown in Table 2. F1 refers to optimised AmB cores (without coating). For comparison purposes, F1 was replicated without the addition of AmB. Formulations F2 and F3 are bi-drug combinations consisting of a core structure with AmB, coated with a single layer containing ITR. HMPCAS, Poloxamer® 188, and Soluplus® were utilised as binding agents.

3.2. Optimisation of AmB cores obtained by wet granulation

The eight experimental runs from the Taguchi design, including independent and dependent variables are displayed in Table 3.

Pareto charts indicated the influence of each factor on each dependent variable (Fig. 1). At the tested conditions, the amount of MCC had a significant effect on yield and dissolution. Pellet manufacturing using a physical mixture of AmB and surfactant exhibited a significantly positive effect in both the yield and the mass ratio, rather than utilising a freeze-dried complex. The use of Soluplus® as a solubilising agent instead of NaDC triggered a higher yield and a higher antifungal activity with a larger particle size; however, NaDC was significantly better in terms of dissolution. The type of PVP, the amount of chitosan and AmB did not exhibit a significant effect on any of the assessed responses.

From the Taguchi design, the three factors which showed the greatest impact on the AmB granule manufacture were: the amount of MCC and the type and amount of surfactant utilised. For this reason, in the Box-Behnken design the amount of MCC, AmB: surfactant ratio, and NaDC: Soluplus® ratio were investigated in more detail. The rest of the components of the formulation were kept constant, using 10 % of chitosan and 25 % of AmB at the optimal amount. Apart from that, a physical mixture was preferred over a freeze-dried system and PVP K17 was the chosen binding agent. The volume of binding solution was removed from the optimisation process as the range evaluated at the Taguchi design led to a wet mass that was very sticky and difficult to granulate.

Independent and dependent variables for the 17 runs in the Box-Behnken design are shown in Table 4. Statistically significant prediction models were found for amount dissolved (after power transformation with λ = 1 and k = 0) and yield, following a 2-factor interaction and a quadratic correlation with the factors with a p-value of 0.038 and 0.002 respectively (Table S1 supplementary material). Correlation models for collected mass fraction and aggregation ratio were not statistically significant (p-value > 0.05 and R-square < 0.8).

MCC showed a positive effect on AmB dissolution. This parameter was also positively influenced when higher amounts of surfactant were used. However, there was no clear indication as to which ratio between Soluplus® and NaDC best influenced dissolution performance (Fig. 2a–c). In terms of yield, total surfactant amount and MCC had a negative impact. Thus, larger amounts of surfactants and MCC resulted

Table 3
Pre-screening Taguchi design matrix for AmB granules. Key: NaDC, sodium deoxycholate. MCC: microcrystalline cellulose. Response 3 (core size ratio) refers to the mass of collected granules larger than 500 μm divided by the mass collected below 500 μm. The antifungal activity was expressed as the inhibition halo against *C. albicans* in mm.

Run	Factor 1	Factor 2	Factor 3	Factor 4	Factor 5	Factor 6	Factor 7	Response 1	Response 2	Response 3	Response 4	Response 5
	MCC (%)	Type of mixture AmB-surfactant	Type of surfactant	Chitosan (%)	AmB (%)	Type of PVP	Volume of PVP (ml)	AmB dissolved at 60 min (%)	Yield (%)	Core size ratio	Antifungal activity *C. albicans* (mm)	Ratio dimer/ monomer
1	25	Physical mixture	NaDC	10	5	K17	8	21.66	76.79	1.86	13.32	0.32
2	25	Freeze-dried	Soluplus®	10	5	K90	4	9.96	75.69	1.54	16.27	0.37
3	5	Physical mixture	Soluplus®	10	25	K17	4	19.91	65.72	1.45	13.2	0.47
4	25	Physical mixture	NaDC	1	25	K90	4	8.57	77.21	1.55	10.37	0.23
5	5	Freeze-dried	NaDC	10	25	K90	8	38.47	47.31	0.56	11.02	0.4
6	5	Physical mixture	Soluplus®	1	5	K90	8	20.34	71.32	2.26	10.32	0.6
7	5	Freeze-dried	NaDC	1	5	K17	4	32.22	41.03	0.14	11.9	0.24
8	25	Freeze-dried	Soluplus®	1	25	K17	8	2.96	67.63	0.97	15.72	0.37

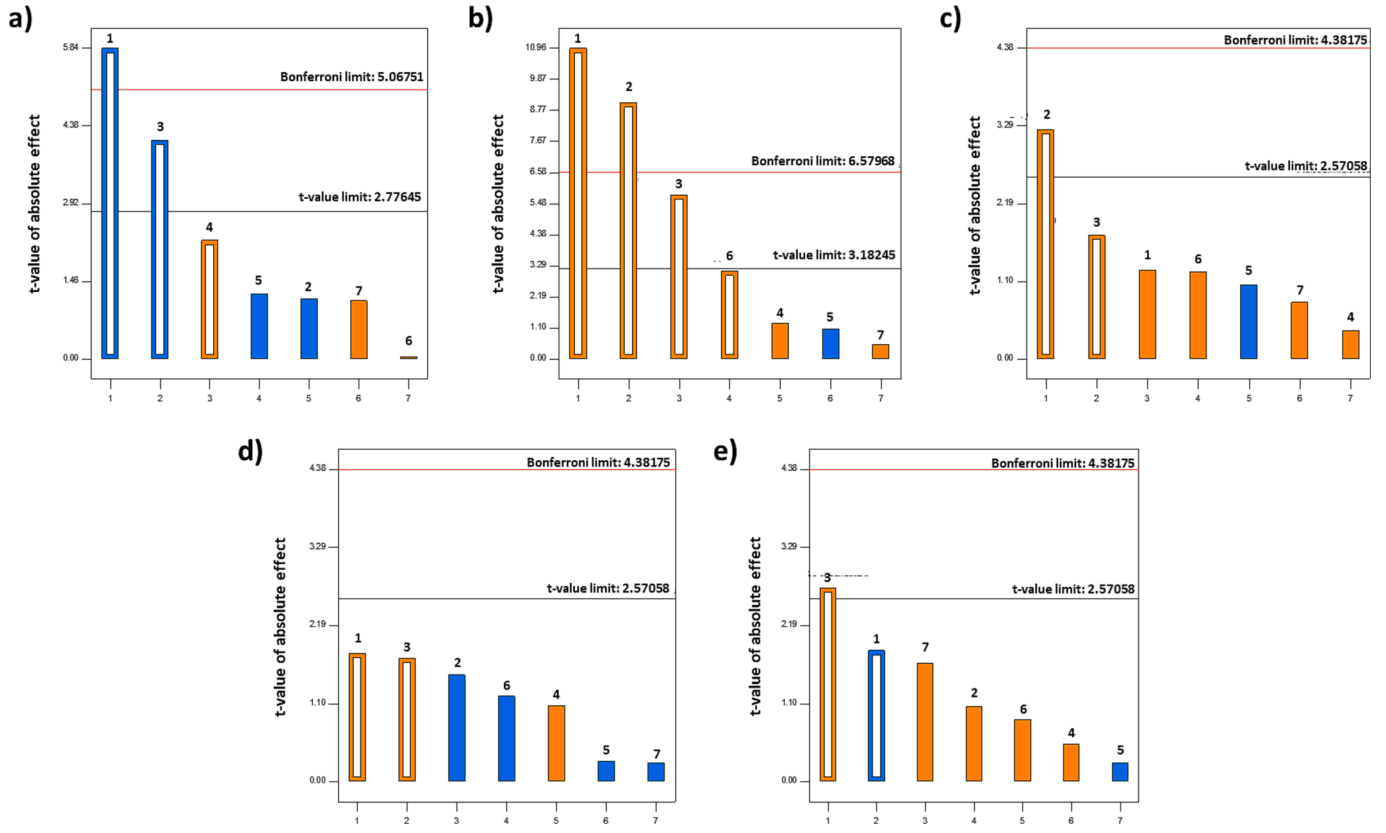

Fig. 1. Pareto charts describing the influence on the seven factors in the Taguchi design: (a) Dissolution rate; (b) Yield; (c) Core size ratio: mass of collected granules greater than 500 μm divided by the mass collected < 500 μm. (d) Antifungal activity against *C. albicans;* (e) Aggregation ratio dimer/monomer. The orange bar represents a positive effect, while the blue bar represents a negative effect. Key: Amount of MCC (1), Type of complex AmB-surfactant (2), Type of surfactant (3), Amount of chitosan (4), Amount of AmB (5), Type of PVP (6), Volume of binding solution (7). Key: Bonferroni limit: effects that are above the Bonferroni limit are almost certainly important; *t*-value limit: effects that are above the *t*-value limit are possibly important. (For interpretation of the references to colour in this figure legend, the reader is referred to the web version of this article.)

in a granulation process with a poorer yield (Fig. 2d–f). Soluplus® showed a better overall performance than NaDC.

The optimised formulation contained 19.6 % of MCC, an AmB: surfactant ratio of 1: 1 (w:w) and a NaDC: Soluplus® ratio of 1:2 (w:w). The final composition of the AmB cores was: inulin (17.64 %), MCC (19.6 %), chitosan (10 %), AmB (25 %), NaDC (6.83 %), Soluplus® (13.64 %), Na_2HPO_4 (5 %) and NaH_2PO_4 (2.25 %). The dependent variables were evaluated for the optimised AmB cores to demonstrate the reliability of the prediction model. The responses were as follows: 38.3 % AmB dissolved after 60 min, a yield of 94.22 %, and core size and aggregation state ratios of 2.61 and 1.76, respectively, which were within the interval confidence predicted for the multilinear regression models.

Table 4
Independent and dependent variables obtained from the experimental runs performed according to the Box-Behnken design. Response 3 (core size ratio) refers to the mass of collected granules greater than 500 μm divided by the mass collected below 500 μm.

Run	Factor 1	Factor 2	Factor 3	Response 1	Response 2	Response 3	Response 4
	Amount of MCC (%)	Ratio AmB: surfactant (w:w)	Ratio NaDC: Soluplus® (w:w)	AmB dissolved at 60 min (%)	Yield (%)	Core size ratio	Ratio dimer/ monomer
1	12.5	1:1	1:1	20.82	90.06	2.4	1.29
2	5	2:1	1:1	17.42	89.13	2.16	0.79
3	20	1:2	1:1	74.21	76.21	2.3	1.76
4	12.5	1:2	1:2	30.2	84.75	2.64	2.75
5	12.5	1:2	2:1	28.75	88.66	2.63	2.97
6	5	1:2	1:1	12.46	80.73	2.39	1.41
7	20	1:1	2:1	7.28	87.52	2.18	1.78
8	5	1:1	2:1	15.48	95.82	2.31	3.38
9	12.5	1:1	1:1	24.49	91.62	2.47	3.18
10	12.5	2:1	1:2	17.26	100	2.1	2.15
11	12.5	1:1	1:1	14.08	93.12	2.32	1.95
12	5	1:1	1:2	16.09	93.62	2.25	3.3
13	20	1:1	1:2	15.8	93.04	2.41	2.17
14	12.5	2:1	2:1	5.12	89.46	2.45	2.72
15	12.5	1:1	1:1	12.46	92.28	2.28	2.53
16	20	2:1	1:1	5.66	88.25	2.55	1.57
17	12.5	1:1	1:1	0.1	86.41	2.27	2.18

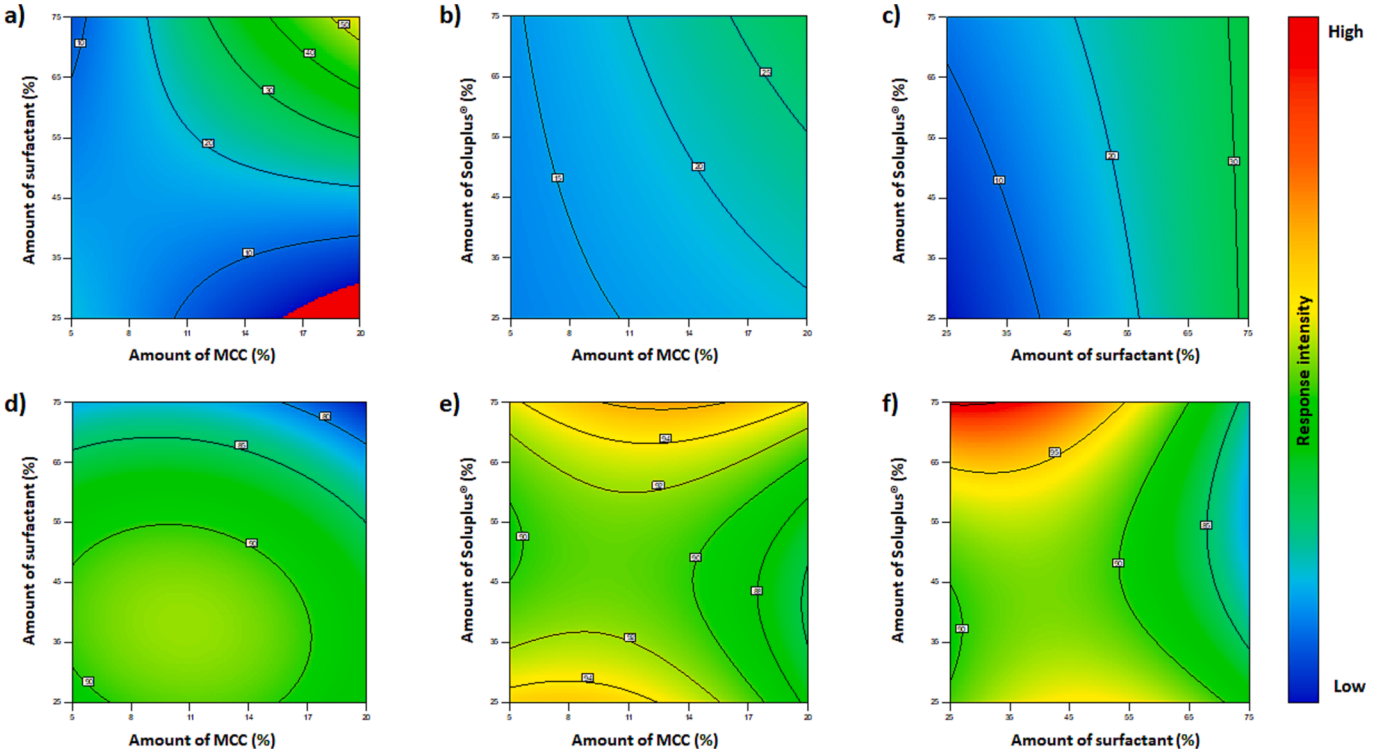

Fig. 2. 2D contour plots showing the influence of the amount of MCC, the amount of surfactant, and the amount of Soluplus® on AmB dissolution (% at 60 min) (a, b, c) and core yield (d, e, f).

Table 5
Physicochemical properties of FDC coated granules. The water content of raw materials is recorded in Table S2 in supplementary material.

Formulation	Composition (binding agent)	Drug	AmB content (%)	ITR content (%)	Water content (%)	D_{50} (μm)	Thickness of coating layer (μm)	Surface area (m^2/ g)
F1	–	–	21.05 ± 1.43	–	7.95 ± 0.03	674.00 ± 11.90	–	2.511 ± 0.008
F2	Soluplus®	ITR	15.07 ± 1.09	9.78 ± 1.73	3.98 ± 0.01	815.10 ± 19.60	70.55 ± 15.75	0.565 ± 0.001
F3	HPMCAS Poloxamer 188	ITR	15.93 ± 1.91	9.77 ± 2.11	2.79 ± 0.08	918.10 ± 9.60	122.05 ± 10.75	0.775 ± 0.005

3.3. Physicochemical characterisation of FDC coated granules

The optimised AmB core was subsequently coated with single coating layers (see Table 2 for composition). The physicochemical characteristics of the three formulations are illustrated in Table 5.

3.3.1. Drug loading

AmB drug loading in the uncoated granules was 21.05 ± 1.43 % (Table 5). During the coating process, AmB drug loading was found to be lower (~15 %) due to a dilution effect caused by the coating layer. ITR drug loading was 9.78 ± 1.73 % and 9.77 ± 2.11 % for F2 and F3, respectively (Table 5).

3.3.2. Calculation of water content by thermogravimetric analysis (TGA)

The water content of the uncoated granules was high (~8 %) (Tables 5 and S2 supplementary material). However, after the coating process, the water content was reduced below 4 % for both formulations.

3.3.3. Surface area and morphology

The surface area of the uncoated granules (2.511 ± 0.008 m^2/g) was significantly diminished after the coating process, showing a 4 to 5-fold reduction in surface area in both cases (Table 5). SEM micrographs of uncoated granules showed quasi-spherical particles with sizes ranging from 500 to 850 μm (Fig. 3a-b). The surface of the uncoated granules was comprised of multiple crystals of smaller size (1–20 μm) which can explain their greater surface area compared to coated formulations that exhibited a smoother appearance (Fig. 3). Granules were also cut in halves to visualise in detail the internal core and the coating layer. In Fig. 3d and 3f the thickness of the coating layer as well as the porous core can be observed.

3.3.4. Powder X-ray diffraction (PXRD)

PXRD analysis of raw materials showed characteristic sharp Bragg peaks for AmB, ITR, NaDC, and Poloxamer 188 indicating that they possess a crystalline nature. MCC and chitosan were semicrystalline, while HMPCAS, Soluplus®, PVPK17, and inulin exhibited a characteristic amorphous halo (Fig. S1 supplementary material). Blank uncoated granules without AmB showed Bragg peaks attributed to NaDC (15.9 2θ) and MCC (22.85 2θ) (Fig. 4a). AmB-loaded granules also showed characteristic Bragg peaks (14.1 and 22.45 2θ) indicating that AmB remained crystalline after the granulation process. The PXRD pattern for the coated granules was similar to that of the AmB uncoated granules, indicating that the crystalline nature was unchanged during the coating process (Fig. 4a and Fig. S1 supplementary material). No additional Bragg peaks were observed in the formulations containing ITR which indicates that spray coating in the presence of Soluplus® and HPMCAS/Poloxamer 188 led to the formation of amorphous solid dispersions of ITR.

3.3.5. Modulated temperature-differential scanning calorimetry (MT-DSC)

DSC thermograms of raw materials showed endothermic events at 172.1 °C, 168.31 °C, and 53.58 °C corresponding to the melting of AmB, ITR, and Poloxamer 188, respectively (Fig. S1a supplementary material). A characteristic dehydration peak was also observed for AmB at 96.5 °C. Apart from that, a dehydration peak was found in all the coated and uncoated formulations due to the moisture content of the granules, as determined by TGA (Table 5 & Fig. S1 supplementary material). F1 (uncoated AmB granules) displayed one endothermic event at 99.2 °C, which was attributed to AmB. The endothermic peak corresponding to the melting of Poloxamer 188 was depressed to lower temperatures (~46 °C). The disappearance of the melting peak of ITR was in good agreement with the PXRD results and was associated with the formation of an amorphous solid dispersion of ITR with the excipients of the coating layer, both Soluplus® and HPMCAS/Poloxamer 188. However, no glass transition was observed for any of the coated granules probably due to the interactions amongst other excipients and signal obscuration.

3.3.6. Fourier-transform infrared spectroscopy (FTIR)

The H-bonding interactions between drug and excipients were studied by FTIR (Fig. 4c & Fig. S2 supplementary material). Sharper peaks were found when the raw materials were analysed separately, in comparison with the spray-coated formulations, which exhibited broadened bands linked with their partial amorphous nature. AmB exhibited characteristic bands of the carbonyl groups, including stretching of the —OH and the stretching of the carboxyl group at 1660 cm^{-1}, 2963 cm^{-1}, and 1422 cm^{-1}, respectively. Displacements of these bands in the spectra of the different formulations indicated that the mentioned groups participate in the H-bonding interactions with other drugs and excipients.

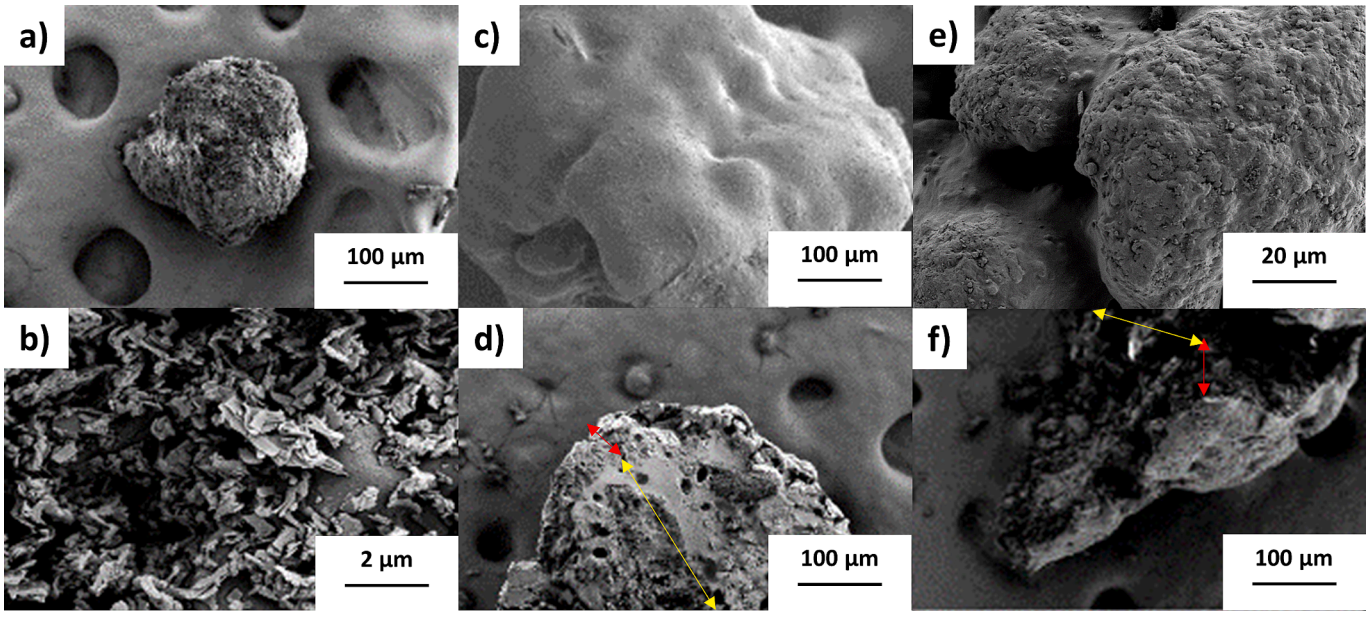

Fig. 3. SEM micrographs of F1 (a, b), F2 (c, d) and F3 (e, f). Key: coating layer (red arrow), core (yellow arrow). (For interpretation of the references to colour in this figure legend, the reader is referred to the web version of this article.)

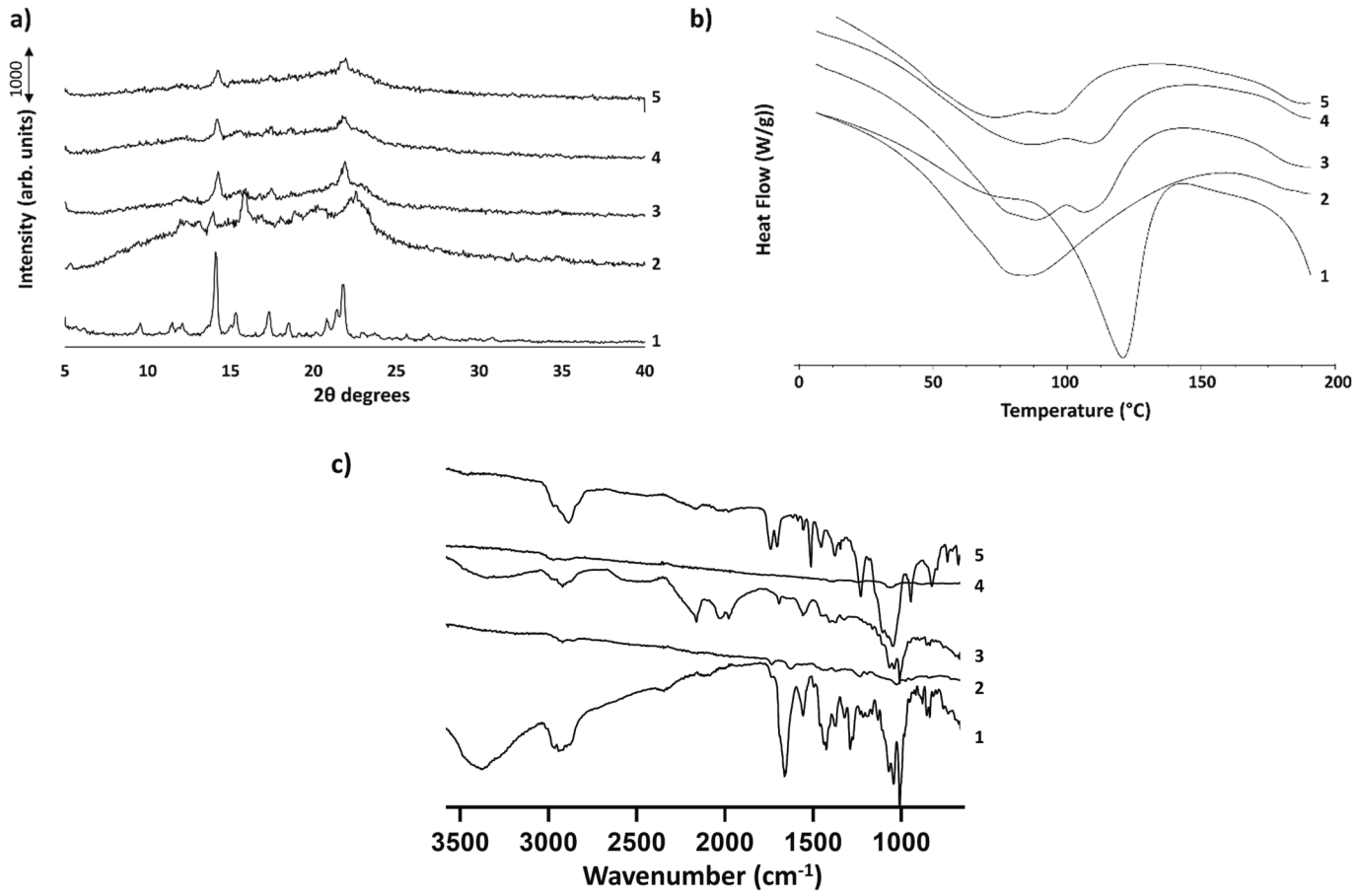

Fig. 4. Physicochemical characterisation of FDC granules: a) PXRD patterns; b) DSC thermograms showing heat flow; c) FTIR spectra. Key: AmB raw material (1), blank core (2), F1 (3), F2 (4) and F3 (5).

3.3.7. *Dynamic vapour sorption (DVS)*

Sorption and desorption isotherms of FDC-coated granules are illustrated in Fig. 5a. The highest water uptake was observed at 90 % RH in F1 (~20 %). Also, the hysteresis was more pronounced in F1. Lower values were observed for all F2 and F3, with a water uptake of 15.5 % and 18 %, respectively. No mass loss was detected in the second sorption and desorption cycle, suggesting that the formulations were stable to recrystallisation. This was confirmed by PXRD performed on samples after DVS analyses that showed no changes in the diffractogram in any of the tested formulations (Fig. 5b).

3.4. *Dissolution studies*

Fig. 6 represents the dissolution profiles of AmB and ITR for the formulations. Uncoated AmB core (F1) showed a pH-dependent release. <1 % AmB was released in the first 30 min of the study, when the pH was set at 1.2, while a faster release was triggered starting at this point when the pH was increased up to 6.8, resulting in 100 % release after 180 min. Dissolution data modelling for F1 showed that AmB release followed Korsmeyer-Peppas kinetics (Table S3 supplementary material). The mechanistic release fitted a Fickian diffusion (with a release exponent

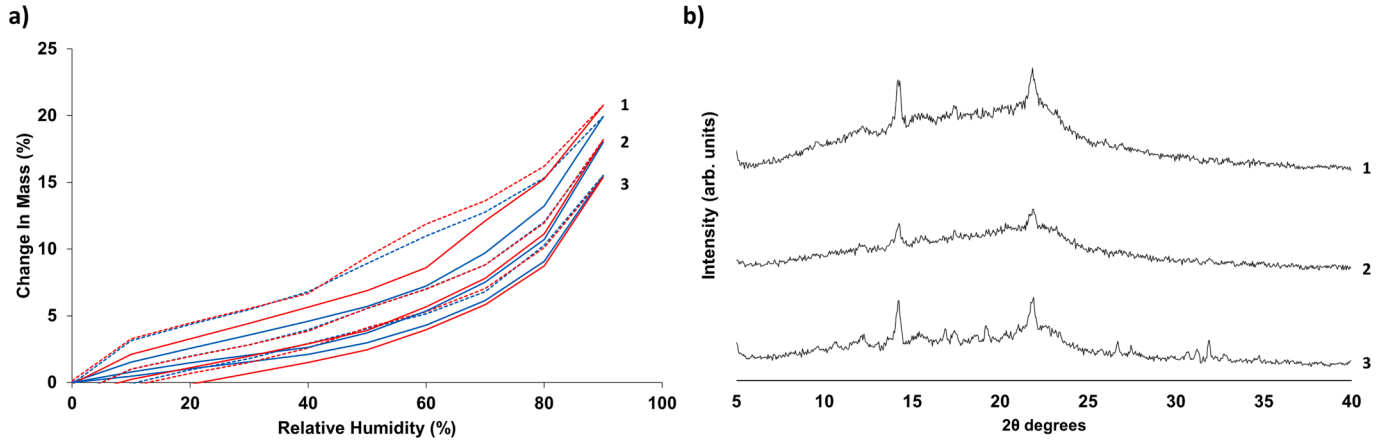

Fig. 5. DVS sorption (solid lines) and desorption (dash lines) isotherms of first (blue lines) and second cycles (red lines) and post-DVS PXRD analyses. Key: F1 (1), F3 (2), F2 (3). (For interpretation of the references to colour in this figure legend, the reader is referred to the web version of this article.)

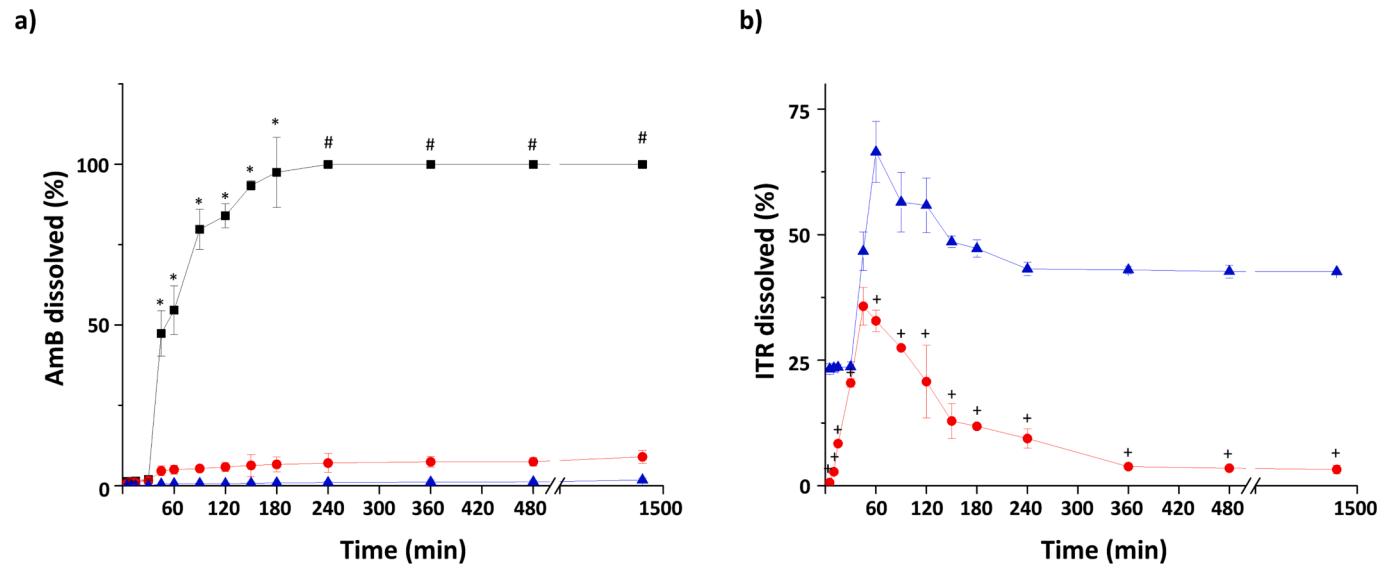

Fig. 6. Cumulative drug release profile for AmB (a) and ITR (b). Key: F1 (black squares), F2 (red circles), F3 (blue triangles). Statistically significant differences between F1 and the other two formulations were represented by *, while # shows statistically significant differences among the three formulations, and statistically significant differences between F2 and F3 are represented by + ($p < 0.05$, one-way ANOVA post-hoc test). (For interpretation of the references to colour in this figure legend, the reader is referred to the web version of this article.)

below 0.43). Granules maintained their shape during the dissolution study for at least 2–3 h. Coated formulations exhibited a slower AmB dissolution rate when compared with F1. These granules exhibited an extremely hindered AmB *in vitro* release from the core (<10 % after 24 h) (Fig. 6a). In this case, AmB release also followed Korsmeyer-Peppas kinetics with a Fickian diffusion mechanism (n < 0.43), which was conditioned by the coating layer that acted as a barrier for AmB release.

ITR showed a dissolution profile characteristic of a supersaturation state [53] with a peak 'spring' at 60 min followed by a parachute effect allowing a window for oral absorption. This supersaturation state was achieved in both formulations coated with ITR (F2 & F3). Based on these results, F1 (uncoated AmB cores) and F2 (coated formulation with ITR and Soluplus®) were selected for further *in vivo* pharmacokinetic testing.

3.5. Accelerated predictive stability studies (APS)

F1 and F2 were selected for long-term and accelerated stability studies (APS). Long-term stability studies showed that all formulations were chemically stable for at least one year (drug content above 95 %) under refrigerated conditions and at room temperature under desiccated conditions (Table 6 and Fig. S3 supplementary material). Humidity had a marked influence on the chemical stability of AmB in the uncoated formulation (F1), with a B term of 0.007. However, a lower value of B term was observed for F2, indicating that the coating layer protected AmB from humidity. AmB and ITR degradation kinetics and activation energies are shown in Table 6. AmB was more sensitive to temperature compared to ITR, which was attributed to its lower activation energy. Degradation of AmB followed a second order and Avrami type kinetic model for F1 and F2, respectively, while ITR degradation kinetics followed a diffusion model.

The prediction models were in good agreement with the long-term experimental results. Overall, formulations exhibited a good chemical stability profile under refrigerated and room temperature desiccated conditions over 1 year.

3.6. In vitro antifungal activity

Results of *in vitro* antifungal activity are shown in Fig. 7a. The *in vitro* activity of the FDC uncoated and coated granules was equivalent to AmB commercial Neosensitab® disks and AmB dissolved in DMSO which is the current gold standard. The inhibition halos of the FDC granules against *C. albicans* and *C.parasilopsis* were well-above 15 mm indicating that both *Candida* spp. were susceptible to the FDC formulations. Lower activity was found against *C. krusei,* although in all cases the inhibition halo was larger than 10 mm, showing that the antifungal effect against this species was concentration-dependent.

3.7. Ex vivo haemolytic toxicity against red blood cells (RBCs)

Haemolytic toxicity data are shown in Fig. 7b. Overall, F2 was the formulation which exhibited the safest profile in red blood cells out of all tested granules with a HC_{50} of 46.43 ± 5.96 μM. However, F3, which also contained AmB and ITR, showed a lower value of HC_{50} (10.13 ±

Table 6
Degradation models of AmB and ITR at the tested conditions of temperature and relative humidity. Key: E_a -activation energy, B term- moisture sensitivity factor.

Formulation	Best fitting model	E_a (kcal/mol)	B term	Predicted stability (years)	Experimental drug content after 1 year at 4 °C and 10 % RH (%)	Experimental drug content after 1 year at 25 °C and 10 % RH (%)
AmB						
F1	Second order	15.049 ± 7.213	0.007 ± 0.002	0.977 ± 0.039	93.607 ± 1.312	91.153 ± 0.464
F2	Avrami	17.527 ± 2.929	0.002 ± 0.001	1.437 ± 0.048	94.436 ± 1.252	91.820 ± 1.100
ITR						
F2	Diffusion	19.059 ± 5.427	0.000 ± 0.000	greater than3 years	99.728 ± 1.073	96.119 ± 0.053

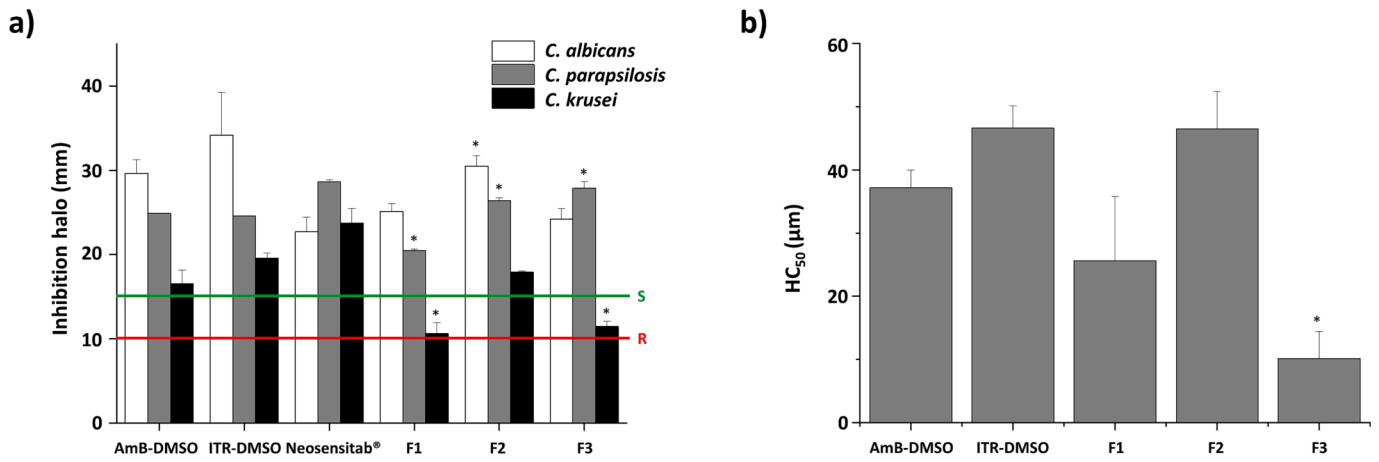

Fig. 7. *In vitro* antifungal activity and haemolytic toxicity of FDC coated granules: a) *in vitro* antifungal activity; b) *in vitro* haemolytic toxicity. In graph *a*, the green line represents *Candida* spp. sensibility (S) while the red line represents resistance (R). In the range between R and S (10–15 mm inhibition halo), the formulations are considered to be concentration-dependent [40]. Statistical significant difference between formulations and AmB-DMSO is represented by * ($p < 0.05$, one-way ANOVA post-hoc test). No statistically significant differences were found among the three controls. (For interpretation of the references to colour in this figure legend, the reader is referred to the web version of this article.)

4.29 µM).

3.8. Oral pharmacokinetic studies

Mouse plasma concentration–time curves of AmB and ITR after single oral administration of FDC granules are illustrated in Fig. 8 and the calculated pharmacokinetic parameters are shown in Table 7.

AmB pharmacokinetic profile was markedly different from ITR, as ITR plasma concentration was found to be much higher. Overall, the t_{max} occurs after 4 h post-administration for both AmB and ITR except for AmB from F2 (coated formulation). ITR showed a greater absorption for F2 than Sporanox®, resulting in a 3.7-fold larger $AUC_{0-\infty}$ and a 2-fold higher Mean Residence Time (MRT). The plasma concentration of AmB from uncoated granules was similar to the AmB suspension.

Cumulative amounts of AmB and ITR after multiple-dose oral administration of FDC granules are shown in Figs. 9 & 10. No statistically significant differences were found between the AmB dispersed in water and the formulations, with the exception of AmB accumulated in lung. Differences were also found in terms of tissue accumulation between AmB and ITR. AmB showed larger drug concentrations in the liver, spleen, and plasma while the highest ITR concentration was found in plasma. The ratio tissue: kidney of AmB after twice-daily oral treatment was calculated to verify the selectivity of AmB towards target organs compared to kidney, due to the high risk of nephrotoxicity associated with the administration of AmB. As a result, AmB (from F1 and F2) was 4.6 and 2-fold more selective towards the liver, 1.5 and 1.7-fold more selective towards the spleen, and 1.2 and 1.3-fold more selective towards the lung, respectively. All formulations were well tolerated, with no signs of gastrointestinal toxicity as mice maintained their body weight during the whole experiment (Fig. S4 supplementary material) [54].

3.9. In vivo toxicological analysis

Results of the toxicological analysis are plotted in Figs. 11 & S5 (supplementary material). The four groups of mice showed high levels of amylase; however, those administered F1 exhibited significantly increased values of amylase in the blood (above 900 U/l), while those

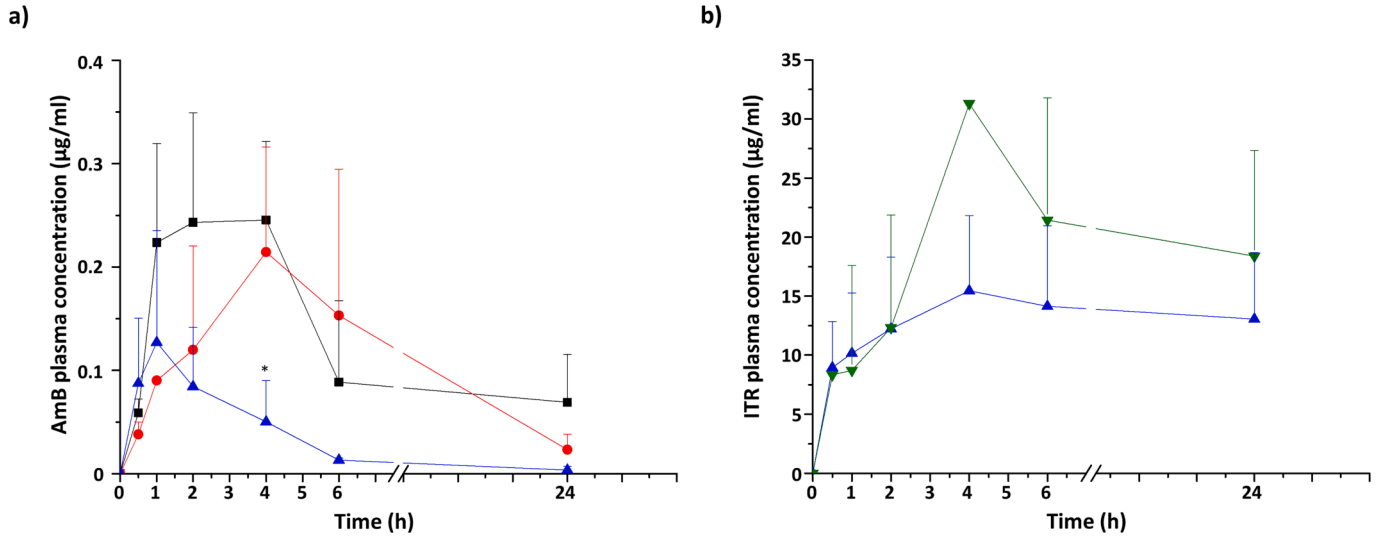

Fig. 8. Plasma levels (±SD) of AmB (a) and ITR (b) after single oral dose administration in CD-1 mice. Key: AmB suspension (black squares), F1 (red circles), F2 (blue triangles), Sporanox® (green inverted triangles). (For interpretation of the references to colour in this figure legend, the reader is referred to the web version of this article.)

Table 7
Pharmacokinetic parameters calculated after single oral administration of FDC granules in CD-1 mice. The dose of AmB was 5 mg/kg and for ITR was 3.25 mg/kg. Values are expressed as average ± SD and were calculated by non-compartimental analysis (PKSolver add-in program). Statistically significant differences as represented as * ($p < 0.05$, one-way ANOVA post-hoc test).

Parameters (units)	AmB			ITR	
	AmB suspension	F1	F2	Sporanox®	F2
C_{max} (μg/ml)	0.25 ± 0.08	0.21 ± 0.03	0.13 ± 0.05 (*)	31.30 ± 6.63	15.46 ± 1.29
t_{max} (h)	4.00 ± 2.22	4.00 ± 1.63	1.00 ± 0.50	4.00 ± 1.63	4.00 ± 1.91
$t_{1/2}$ (h)	8.72 ± 2.18	6.16 ± 3.98	3.96 ± 2.49	12.36 ± 2.93	27.03 ± 2.98 (*)
λ (h^{-1})	0.08 ± 0.03	0.17 ± 0.11	0.42 ± 0.56	0.04 ± 0.03	0.03 ± 0.00
AUC_{0-t} (μg/ml*h)	2.61 ± 0.82	2.00 ± 1.46	0.50 ± 0.12 (*)	298.55 ± 20.16	541.21 ± 57.93 (*)
$AUC_{0-\infty}$ (μg/ml*h)	3.18 ± 0.97	2.35 ± 1.30	0.53 ± 0.15	354.38 ± 54.22	1299.33 ± 122.03 (*)
$MRT_{0-\infty}$ (μg/ml*h)	13.44 ± 2.33	10.50 ± 4.54	5.09 ± 3.11	19.02 ± 6.67	40.28 ± 4.43 (*)
V_d (l)	2.52 ± 1.50	9.73 ± 0.00	9.14 ± 3.74 (*)	0.04 ± 0.01	0.03 ± 0.00
Cl (ml/h)	307.35 ± 48.00	571.98 ± 19.07	1395.17 ± 165.54 (*)	1.49 ± 1.04	0.89 ± 0.43

given F2 showed the lowest values (~500 U/l). Furthermore, increased amylase values were visually evident when tissue samples were collected, specifically liver and spleen, as the shape and the colour of these organs had been modified after treatment. Apart from that, F1 administration also resulted in significantly increased levels of Na^+ (~155 mmol/l), while animals given F2 showed the lowest values of Na^+, being the only group in the optimal range for this cation (~145 mmol/l). No other significant differences were observed among the other biochemical parameters.

4. Discussion

To the best of our knowledge, this is the first report of an orally administered formulation combining AmB with other antifungal drugs. Two AmB-ITR-loaded FDC formulations were manufactured by wet granulation followed by spray-coating. In addition, a single-drug formulation containing AmB was obtained by wet granulation [55]. In terms of the excipients utilised, inulin was incoporrated so as to enhance the tolerability of pellets when orally administered, as it has been reported to prevent the gastrointestinal toxicity caused by AmB due to a prebiotic effect which is beneficial for enterocytes and intestinal flora [56,57]. MCC was utilised as a disintegrant, and showed a positive effect on dissolution rate, possibly due to it allowing acceleration of drug diffusion through the pellets [58]. Chitosan was added due to its mucoadhesive properties that leads to a greater oral bioavailability of AmB [59]. Both NaDC and Soluplus® were selected as solubilising agents, promoting dissolution rate at higher concentrations. Also, PVP K17 was preferably utilised as a binder, as the use of PVP K90 may hinder AmB release due to its larger molecular weight. The amount of MCC and surfacant and the type of surfactant played a key role in dissolution and drug efficacy. A larger amount of AmB was added to the core (25 % versus 5 %) when formulation optimisation was undertaken, given that oral absorption is limited and enough drug should reach the target tissues to elicit a pharmacological effect. Regarding manufacturing, a physical mixture between drug and excipient was determined to be preferable than a freeze-dried powder, as a higher yield was achieved with the former, producing larger granules with a reduced risk of attrition, which is beneficial when utilising spray coating.

SEM images confirmed that coated and uncoated formulations possessed a different morphology. F1 exhibited a rough structure made of microscopic crystals; however, coated pellets (F2 and F3) showed a smoother surface. When these pellets were cut in half, the internal structure was very similar to F1, indicating the differences were due to the coating layer than any changes that might have occurred during the coating process.

Dissolution studies showed that the uncoated core (F1) allowed the fastest AmB release among the three formulations (100 % AmB release after 3 h). AmB release was found to be pH-dependent, as it was hindered during the first 30 min when the pH of the dissolution medium was pH 1.2. This is representative of what could happen *in vivo,* as the drug should remain unreleased while residing in the stomach, and drug release should take place once the formulation reaches the intestine. This is of special importance, considering that AmB degradation kinetics in the acidic pH of the stomach is fast, and hence, it is preferable that release takes place in the intestine. Dissolution data modelling showed that AmB release followed a Korsmeyer-Peppas kinetics model, fitted to a Fickian diffusion ($n < 0.43$), which could be explained by the quasi-spherical shape of the granules, which was maintained during the dissolution study for at least 2 h. However, coated formulations exhibited a slower AmB dissolution rate. AmB *in vitro* release was hindered by the coating layer, which acted as a barrier for AmB release. In this case, AmB release also followed a Korsmeyer-Peppas diffusion mechanism ($n < 0.43$). Nevertheless, ITR showed a very different *in vitro* release behaviour. When combining AmB and ITR, a supersaturation state with a 'spring' effect of ITR was found at 60 min [60,61]. This means that ITR should show a burst release at the early stages of administration while AmB remains unreleased, allowing a window for oral absorption.

Stability studies demonstrated that the formulations were chemically stable for at least one year under refrigerated conditions and at room temperature if stored under desiccated conditions. Relative humidity played a marked role in the chemical stability of AmB, primarily in F1 because of the absence of a coating layer. This coating layer acted as a moisture protective barrier in F2, and hence, this formulation was less susceptible to degradation triggered by moisture. However, the humidity did not have a large influence on the ITR chemical stability. AmB was also more sensitive to temperature compared to ITR, as shown by the values of activation energy. Degradation of AmB in F1 followed second-order kinetics, while F2 degradation followed an Avrami and diffusion model for AmB and ITR, respectively. This means that, in F1, AmB degradation depended on drug concentration, but it was also promoted by other components of the core [62]. However, the coating layer modified the degradation kinetics of AmB, as, in the coated formulation, initially, the AmB degradation process is very slow, but once degradation occurs, the process becomes exponential [63], hence it is important to avoid the propagation of the degradation. Meanwhile, ITR degradation takes place due to an autocatalytic reaction which occurs by an immediate supersaturation of water [64]. Having this knowledge, packaging can be selected appropriately to ensure that the propagation step does not take place. Based on all of the above, foil-foil packaging materials would be recommended, as well as storage under refrigerated and desiccated conditions to enhance the shelf-life, while sachets packed inside aluminum blister packs would be ideal for commercialisation [65]. The prediction models were in good agreement with the long-term experimental results. The models obtained were considered non-conservative for both drugs, as the models suggested a higher drug content after 3 years than the experimental drug content obtained at that time point.

Antifungal activity was also assessed by measuring the inhibition halos in the agar diffusion assay. The inhibition halos of the formulations against *C. albicans* and *C. parapsilosis* were well-above 15 mm, indicating that both species were susceptible to the formulations. However, a lower activity was found against *C. krusei,* which is a

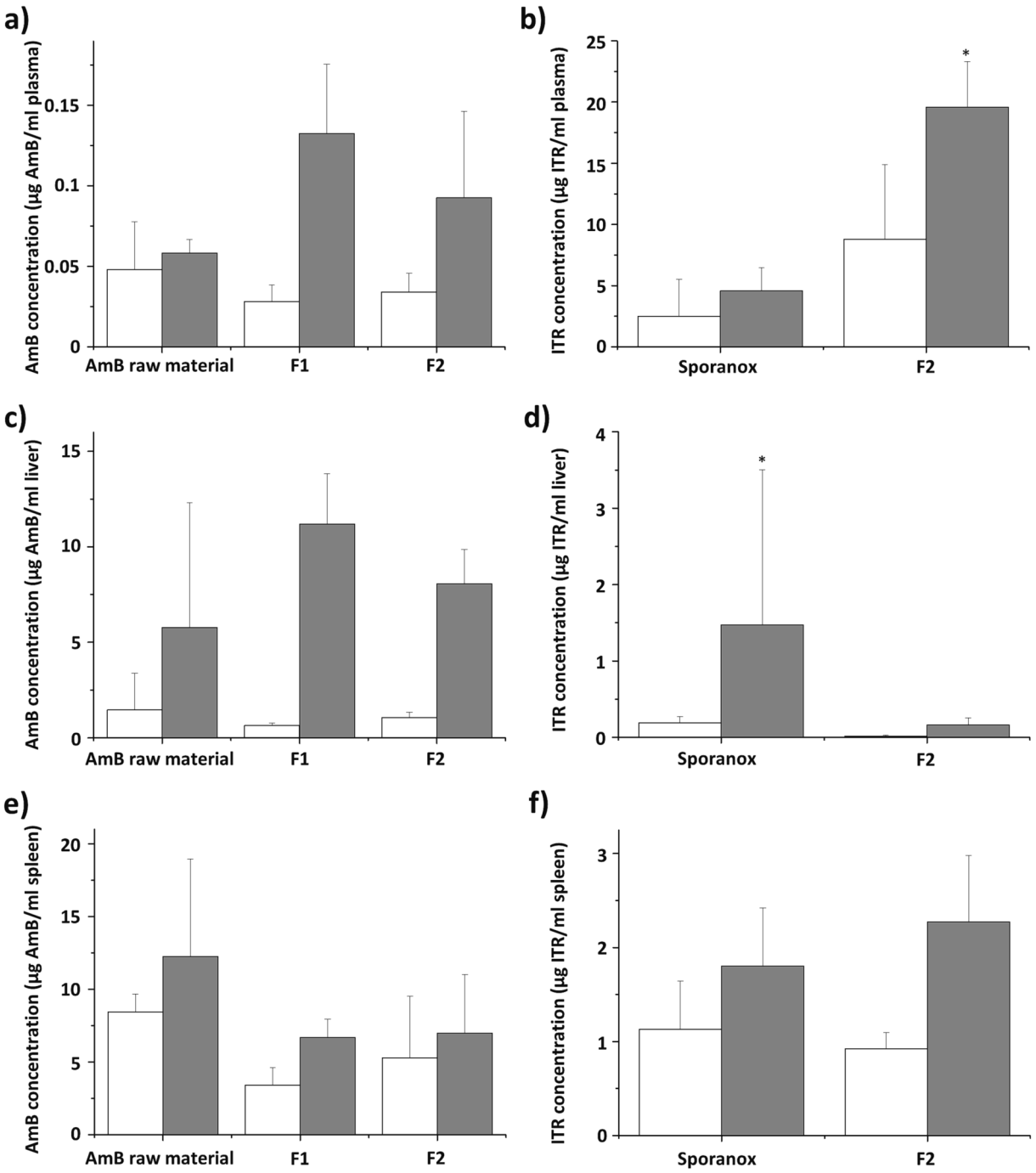

Fig. 9. Multiple dose oral administration of FDC granules: AmB and ITR concentrations (±SD) in plasma (a, b), liver (c, d), and spleen (e, f). Key: AmB and ITR concentrations at 24 h following the completion of once daily for 5 days oral treatment course of 5 mg/kg and 3.25 mg/kg of AmB and ITR, respectively (white), and AmB and ITR concentration at 12 h following the completion of twice daily for 5 days oral treatment course at the same doses (gray). Statistically significant difference is represented by * ($p < 0.05$ one-way ANOVA post-hoc test).

multidrug-resistant opportunistic fungal pathogen [66]. Nevertheless, F2 showed an inhibition halo above 15 mm, indicating that this formulation could potentially be useful to treat this infection, as an enhanced effect between AmB and ITR was found. Regarding toxicity, F2 (AmB-ITR pellets using Soluplus® in the coating) showed the highest HC_{50} value, which means it is the safest formulation. Thus, F2 showed the most promising results in terms of efficacy and toxicity.

Based on all of the above, F1 (uncoated AmB granules) and F2 (coated AmB granules with ITR and Soluplus®) were selected for further *in vivo* testing. The pharmacokinetic profile of AmB was markedly different from ITR. The latter was characteristic of longer periods of circulation in the bloodstream, resulting in much greater plasma concentrations than AmB. In contrast, AmB, as reported by other authors [59,67], is rapidly removed from the blood, being accumulated in tissues, mainly in liver, spleen, and lung. Overall, the reported t_{max} (4 h post-administration) was attributed to the controlled release of the drug from the granules over time. Also, both drugs may have suffered from enterohepatic circulation, being excreted back to the intestinal tract from the bile, and hence, a reabsorption process at later times may have occurred. On the other hand, ITR from F2 showed a greater absorption than ITR from Sporanox®, possibly attributed to the 'spring' effect which was seen in the *in vitro* dissolution studies. Apart from that, the

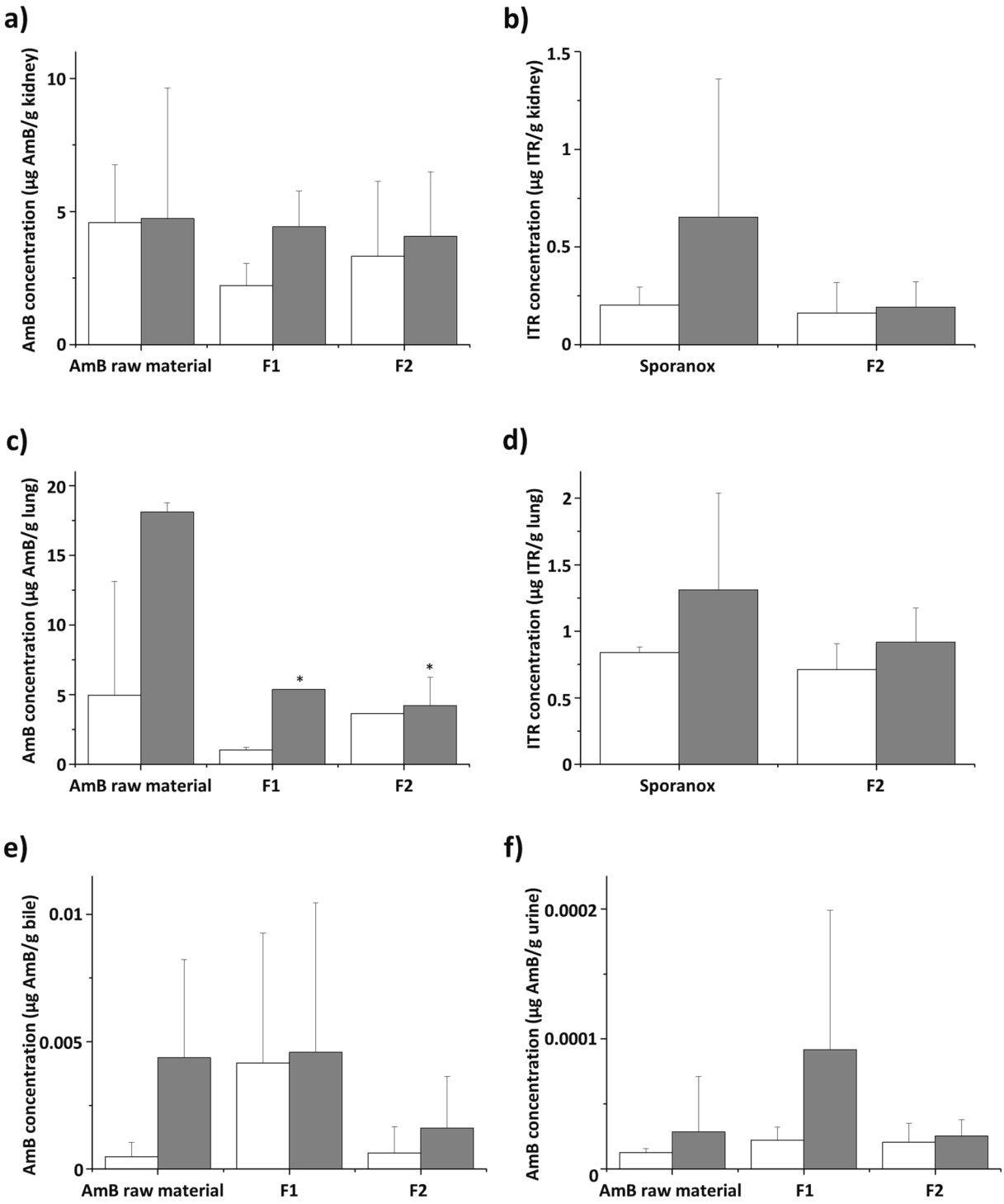

Fig. 10. Multiple dose oral administration of FDC granules: AmB and ITR concentrations (±SD) in kidney (a, b) and lung (c, d) and AmB concentrations in bile (e) and urine (f). Key: AmB and ITR concentrations at 24 following the completion of once daily for 5 days oral treatment course of 5 mg/kg and 3.25 mg/kg of AmB and ITR, respectively (white), and AmB and ITR concentrations at 12 h following the completion of twice daily for 5 days oral treatment course at the same doses (gray). Statistical significant difference is represented by * ($p < 0.05$ one-way ANOVA post-hoc test).

highest ITR concentration was found in plasma, meaning that it tended to recirculate in the bloodstream, in contrast to AmB being translocated to tissues. However, the solubilisation of ITR from the coating layer could have been partial, and hence, AmB release from the core was hindered, especially at later time points when the ITR supersaturation state no longer exists, limiting the oral absorption of AmB compared to the F1 formulation. The plasma concentration of AmB from uncoated pellets was similar to the AmB suspension. It is known that both drugs have a high protein plasma binding (above 90 %), specifically to serum albumin [68–70]. Although these data would suggest that both drugs would remain in the bloodstream, as it is known that only free drugs are able to translocate from blood to organs [71], it has been previously reported that AmB can be uptaken via the enterocytes and Peter's patches. This would lead to an AmB transport from the gut-associated lymphoid tissue via lymphatic vessels, where macrophages can uptake AmB and deliver the drug to organs of the reticuloendothelial system,

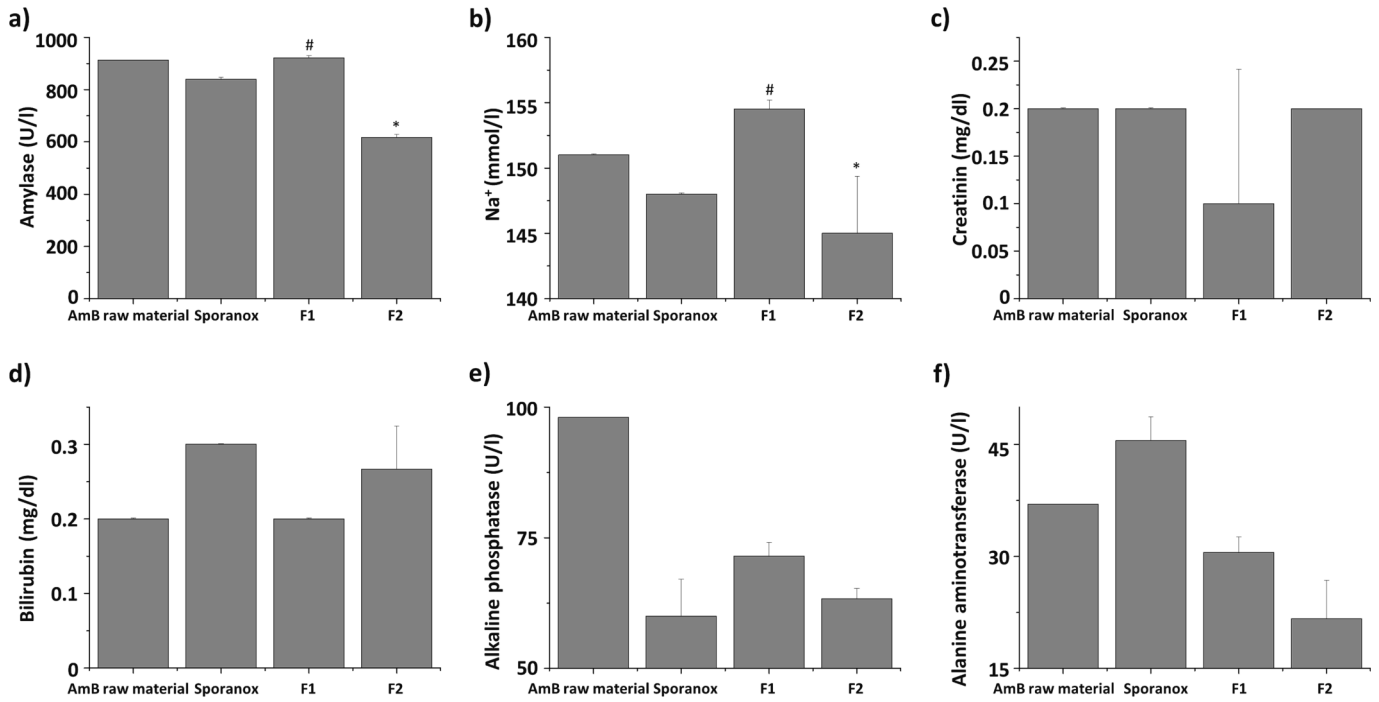

Fig. 11. Toxicology after 5-days twice daily administration of AmB granules and control formulations: (a) Amylase levels (U/l) (±SD); (b) Na^+ levels (mmol/l) (±SD); (c) Creatinin levels (mg/dl) (±SD); (d) Bilirubin levels (mg/dl) (±SD); (e) Alkaline phosphatase (U/l) (±SD); (f) Alanine aminotransferase (U/l) (±SD). Statistically significant differences are represented by * (formulations vs AmB raw material suspension, $p < 0.05$) and # (formulations vs Sporanox®, $p < 0.05$).

such as the liver, spleen, and lung, as previously reported [59]. This could be caused due to the formation of micelles with the excreted bile salts in the gastrointestinal tract [72]. A poor translocation of ITR to these tissues has also been reported in the literature [73], although it could be targeted toward muscle, skin, and fat. When comparing the cumulative amounts of AmB in tissues, the drug was found as follows: liver > spleen > lung > kidney. This could be therapeutically advantageous to treat liver fungal infections caused by *Candida* spp., which are common in oncohematologic patients with severe and prolonged neutropenia [74], but also due to its lower toxicity, as AmB is not highly translocated towards the kidney, avoiding severe nephrotoxicity [20,22,23]. This low translocation in kidneys could be associated with lower renal toxicity. All formulations were well tolerated, with no signs of gastrointestinal toxicity which had been previously reported in the literature when administering AmB orally [20,54]. This was thought to be prevented using inulin which avoided damage to the enterocytes. When comparing oral AmB formulations previously described in the literature with these pellets [59,75,76], in a twice-daily administration regimen, delivery towards target tissues ranged from 4.4 μg AmB/g kidney to 11.2 μg AmB/g liver after oral administration of F1 and from 3.3 μg AmB/g kidney to 8.1 μg AmB/g liver after oral administration of F2. As a result, tissue distribution was enhanced 1.9 and 1.3-fold in the liver for F1 and F2, respectively, while no significant increase was found in other tissues in comparison with previous research [59].

Regarding toxicity, after twice-daily oral administration of these formulations for 5 days, increased values of amylase were found in blood (above 500 U/l in all cases), which might be indicative of acute pancreatitis [77]. Pancreatitis can lead to complications in the digestive system, which could also be observed when tissue samples were collected, as the shape and the colour of these organs had been altered. Apart from that, F1 also showed significantly increased levels of Na^+, which could be related to dehydration induced by several causes, such as not drinking enough water, diarrhea, or kidney malfunction [78]. As animals had free access to food and water during the 5-days treatment course, it is very unlikely that dehydration occurred. Also, no signs of diarrhea were observed, so probably the nephrotoxicity characteristic of AmB might have led to hypernatremia [22]. However, Na^+ levels were in the optimal range (135–145 mmol/l) after the administration of F2, indicating that combining antifungals may help in reducing nephrotoxicity caused by AmB. Moreover, other biochemical alterations were found, including a decrease in blood urea nitrogen (BUN) (~17 g/dl) and alanine aminotransferase (ALT) (<30 U/l) and increased levels of bilirubin (~0.2 mg/dl) and alkaline phosphatase (ALP) (<80 U/l). These altered values could be indicative of biochemical abnormalities consistent with acute drug-induced liver injury. As liver failure might lead to a negative outcome of the treatment, while once daily administration might not be sufficient to treat fungal infections due to a reduced drug content found in tissues, a suitable alternative should be found to administer these formulations. Replacing twice-daily oral administration for 5 days with a once-daily regimen for 10 days may represent a good choice of dosage regimen, based on previous research [10].

5. Conclusions

Oral FDC of AmB granules could be an advantageous alternative to intravenous administration of AmB being a more 'patient-friendly' treatment without the need for patient hospitalisation which is not a convenient alternative in developing countries. The engineered formulations were stable for at least 1 year, but also effective against the tested species of *Candida* spp., including *C. krusei* when AmB was combined with ITR. These results are very advantageous for the treatment of systemic fungal infection in clinical practice. The use of coating layers sustained the release of AmB from 3 to 24 h, while ITR exhibited a 'spring' release effect at early stages. *In vivo* studies demonstrated the translocation of AmB to liver (11.2 μg AmB/g liver after twice daily administration during 5 consecutive days), which could be potentially advantageous to treat severe liver fungal infections, including *Candida* spp. and *Aspergillus* spp, although no significant improvement has been found compared to the AmB dispersed in water. This can be attributed to the lower intestinal pH of rodents compared to humans which questions their applicability on enteric-coated drug carriers [79]. Nevertheless, the biochemical alterations found in the toxicity studies suggested that a

twice-daily administration of the treatment for 5 days might not be ideal and replacing this regimen for a once-daily oral administration for 10 days would be a safer alternative to consider, but further experiments need to be carried out. Concentrations achieved in tissues after multiple administration were greater than the minimum inhibitory concentration for AmB and ITR, and hence, it is expected than the novel AmB-ITR fixed- dose formulation would be effective against systemic fungal infections.

Declaration of Competing Interest

The authors declare that they have no known competing financial interests or personal relationships that could have appeared to influence the work reported in this paper.

Data availability

Data will be made available on request.

Acknowledgements

This work was funded by Banco de Santander-Universidad Complutense (project PR26/16-20355) and by the Iberoamerican Union of Universities (project ENF03/2017), awarded to F. Bolás-Fernández.

A.M. Healy acknowledges a Science Foundation Ireland grant co-funded under the European Regional Development Fund (SFI/12/RC/2275_P2). This study has been also funded by the Ministry of Science and Innovation (award PID2021-126310OA-I00 to Dolores Serrano).

Appendix A. Supplementary material

Supplementary data to this article can be found online at https://doi.org/10.1016/j.ejpb.2023.01.003.

References

[1] J. Fortún, Antifungal therapy update: new drugs and medical uses, Enferm. Infecc. Microbiol. Clin. 29 (Suppl. 5) (2011) 38–44.
[2] J. van Griensven, M. Boelaert, Combination therapy for visceral leishmaniasis, Lancet (London, England) 377 (2011) 443–444.
[3] I.W. Yerbanga, S. Nakanabo Diallo, T. Rouamba, O. Denis, H. Rodriguez-Villalobos, I. Montesinos, S. Bamba, A systematic review of epidemiology, risk factors, diagnosis, antifungal resistance, and management of invasive aspergillosis in Africa, J. Med. Mycol. 33 (2023).
[4] Á. Medina, La resistencia a los antibióticos y la falta de interés de la industria farmacéutica, Infectio 18 (2014).
[5] A.R. White, , on behalf of the BSAC Working Party on The Urgent Need: Regenerating Antibacterial Drug Discovery and Development, M. Blaser, O. Carrs, G. Cassell, N. Fishman, R. Guidos, S. Levy, J. Powers, R. Norrby, G. Tillotson, R. Davies, S. Projan, M. Dawson, D. Monnet, M. Keogh-Brown, K. Hand, S. Garner, D. Findlay, C. Morel, R. Wise, R. Bax, F. Burke, I. Chopra, L. Czaplewski, R. Finch, D. Livermore, L.J.V. Piddock, T. White, Effective antibacterials: at what cost? The economics of antibacterial resistance and its control, J. Antimicrob. Chemother. 66 (2011) 1948–1953.
[6] D.S. Bell, Combine and conquer: advantages and disadvantages of fixed-dose combination therapy, Diabetes Obes. Metab. 15 (2013) 291–300.
[7] P. Mazón, E. Galve, J. Gómez, M. Gorostidi, J.L. Górriz, J.D. Mediavilla, Medical expert consensus in AH on the clinical use of triple fixed-dose antihypertensive therapy in Spain, Hipertens Riesgo Vasc 33 (2016) 133–144.
[8] R. Fernández-García, M. Prada, F. Bolás-Fernández, M.P. Ballesteros, D.R. Serrano, Oral fixed-dose combination pharmaceutical products: industrial manufacturing versus personalized 3D printing, Pharm. Res. 37 (2020) 132.
[9] A. Mazza, L. Schiavon, M. Zuin, S. Lenti, E. Ramazzina, D. Rubello, E. Casiglia, Effects of the antihypertensive fixed-dose combinations on an early marker of hypertensive cardiac damage in subjects at low cardiovascular risk, Am. J. Hypertens. 29 (2016) 969–975.
[10] S.S. Kim, I.J. Kim, K.J. Lee, J.H. Park, Y.I. Kim, Y.S. Lee, S.C. Chung, S.J. Lee, Efficacy and safety of sitagliptin/metformin fixed-dose combination compared with glimepiride in patients with type 2 diabetes: a multicenter randomized double-blind study, J. Diabetes 9 (2017) 412–422.
[11] G.T. Everson, K.D. Sims, P.J. Thuluvath, E. Lawitz, T. Hassanein, M. Rodriguez-Torres, T. Desta, T. Hawkins, J.M. Levin, F. Hinestrosa, V. Rustgi, H. Schwartz, Z. Younossi, L. Webster, N. Gitlin, T. Eley, S.P. Huang, F. McPhee, D.M. Grasela, D. F. Gardiner, Daclatasvir + asunaprevir + beclabuvir ± ribavirin for chronic HCV genotype 1-infected treatment-naive patients, Liver Int. 36 (2016) 189–197.
[12] Fungizone 50 mg powder for sterile concentrate, Available from: https://www.medicines.org.uk/emc/product/10716/smpc#gref (retrieved on: 1st December 2022).
[13] S. Kumari, V. Kumar, R.K. Tiwari, V. Ravidas, K. Pandey, A. Kumar, Amphotericin B: a drug of choice for visceral leishmaniasis, Acta Trop. 235 (2022).
[14] AmBisome, data sheet, Available from: https://cima.aemps.es/cima/dochtml/ft/61117/FT_61117.html (retrieved on: 1st December 2022).
[15] F.F. Tuon, L.R. Dantas, R.M. de Souza, V.S.T. Ribeiro, V.S. Amato, Liposomal drug delivery systems for the treatment of leishmaniasis, Parasitol. Res. 121 (2022) 3073–3082.
[16] D.N. Mario, J. Guarro, J.M. Santurio, S.H. Alves, J. Capilla, In vitro and in vivo efficacy of amphotericin B combined with posaconazole against experimental disseminated sporotrichosis, Antimicrob. Agents Chemother. 59 (2015) 5018–5021.
[17] R.A. Larsen, M. Bauer, A.M. Thomas, J.R. Graybill, Amphotericin B and fluconazole, a potent combination therapy for cryptococcal meningitis, Antimicrob. Agents Chemother. 48 (2004) 985–991.
[18] F.C. Odds, Fluconazole plus amphotericin B combinations are not contraindicated and may add benefit for the treatment of candidemia, Clin. Infect. Dis. 36 (2003) 1229–1231.
[19] M.S. Ching, K. Raymond, R.W. Bury, M.L. Mashford, D.J. Morgan, Absorption of orally administered amphotericin B lozenges, Br. J. Clin. Pharmacol. 16 (1983) 106–108.
[20] J.J. Torrado, D.R. Serrano, I.F. Uchegbu, The oral delivery of amphotericin B, Ther. Deliv. 4 (2013) 9–12.
[21] D. Desai, J. Wang, H. Wen, X. Li, P. Timmins, Formulation design, challenges, and development considerations for fixed dose combination (FDC) of oral solid dosage forms, Pharm. Dev. Technol. 18 (2013) 1265–1276.
[22] R. Fernández-García, E. de Pablo, M.P. Ballesteros, D.R. Serrano, Unmet clinical needs in the treatment of systemic fungal infections: the role of amphotericin B and drug targeting, Int. J. Pharm. 525 (2017) 139–148.
[23] J.J. Torrado, R. Espada, M.P. Ballesteros, S. Torrado-Santiago, Amphotericin B formulations and drug targeting, J. Pharm. Sci. 97 (2008) 2405–2425.
[24] R. Fernández-García, J.C. Muñoz-García, M. Wallace, L. Fabian, E. González-Burgos, M.P. Gómez-Serranillos, R. Raposo, F. Bolás-Fernández, M.P. Ballesteros, A.M. Healy, Y.Z. Khimyak, D.R. Serrano, Self-assembling, supramolecular chemistry and pharmacology of amphotericin B: Poly-aggregates, oligomers and monomers, J. Control. Release 341 (2022) 716–732.
[25] A. Kozyra, N.A. Mugheirbi, K.J. Paluch, G. Garbacz, L. Tajber, Phase diagrams of polymer-dispersed liquid crystal systems of itraconazole/component immiscibility induced by molecular anisotropy, Mol. Pharm. 15 (2018) 5192–5206.
[26] J.W. Mouton, A. van Peer, K. de Beule, A. Van Vliet, J.P. Donnelly, P.A. Soons, Pharmacokinetics of itraconazole and hydroxyitraconazole in healthy subjects after single and multiple doses of a novel formulation, Antimicrob. Agents Chemother. 50 (2006) 4096–4102.
[27] A. Kane, D.A. Carter, Augmenting azoles with drug synergy to expand the antifungal toolbox, Pharmaceuticals (Basel) 15 (2022).
[28] Itraconazole 100 mg capsules, data sheet, Available from: https://cima.aemps.es/cima/dochtml/ft/65773/FT_65773.html (retrieved on: 1st December 2022).
[29] J.M. Lestner, S.A. Roberts, C.B. Moore, S.J. Howard, D.W. Denning, W.W. Hope, Toxicodynamics of itraconazole: implications for therapeutic drug monitoring, Clin. Infect. Dis. 49 (2009) 928–930.
[30] C. Anis Yohana, S. Sriwidodo, A. Marline, Microcrystalline cellulose as pharmaceutical excipient, in: A. Usama, A. Juber (Eds.), Pharmaceutical Formulation Design, IntechOpen, Rijeka, 2019, pp. 3.
[31] M. Yang, S. Xie, Q. Li, Y. Wang, X. Chang, L. Shan, L. Sun, X. Huang, C. Gao, Effects of polyvinylpyrrolidone both as a binder and pore-former on the release of sparingly water-soluble topiramate from ethylcellulose coated pellets, Int. J. Pharm. 465 (2014) 187–196.
[32] B.K. Rasool, S.A. Fahmy, O.W. Galeel, Impact of chitosan as a disintegrant on the bioavailability of furosemide tablets: in vitro evaluation and in vivo simulation of novel formulations, Pak. J. Pharm. Sci. 25 (2012) 815–822.
[33] J.-H. Weitkamp, J.J. Nania, Chapter 6 - Infectious Diseases, in: G.M. Fenichel (Ed.), Neonatal Neurology (Fourth Edition), Churchill Livingstone, Edinburgh, 2007, pp. 109–141.
[34] A. Eissens, G. Bolhuis, W. Hinrichs, H. Frijlink, Inulin as filler-binder for tablets prepared by direct compaction, Eur. J. Pharm. Sci.: Off. J. Eur. Federat. Pharm. Sci. 15 (2002) 31–38.
[35] J. Aisara, P. Wongputtisin, S. Deejing, C. Maneewong, K. Unban, C. Khanongnuch, P. Kosma, M. Blaukopf, A. Kanpiengjai, Potential of Inulin-Fructooligosaccharides Extract Produced from Red Onion (Allium cepa var. viviparum (Metz) Mansf.) as an Alternative Prebiotic Product, Plants (Basel) 10 (2021).
[36] R. Fernández-García, A. Lalatsa, L. Statts, F. Bolás-Fernández, M.P. Ballesteros, D. R. Serrano, Transferosomes as nanocarriers for drugs across the skin: Quality by design from lab to industrial scale, Int. J. Pharm. 573 (2020), 118817.
[37] A.-R. Alao, M. Konneh, Application of Taguchi and Box-Behnken designs for surface roughness in precision grinding of silicon, Int. J. Precis. Technol. 2 (2011) 21–38.
[38] M. Rolón, D.R. Serrano, A. Lalatsa, E. de Pablo, J.J. Torrado, M.P. Ballesteros, A. M. Healy, C. Vega, C. Coronel, F. Bolás-Fernández, M.A. Dea-Ayuela, Engineering oral and parenteral amorphous amphotericin B formulations against experimental Trypanosoma cruzi infections, Mol. Pharm. 14 (2017) 1095–1106.
[39] D.R. Serrano, R. Fernandez-Garcia, M. Mele, A.M. Healy, A. Lalatsa, Designing fast-dissolving orodispersible films of amphotericin B for oropharyngeal candidiasis, Pharmaceutics 11 (2019).

[40] H.K. Ruiz, D.R. Serrano, M.A. Dea-Ayuela, P.E. Bilbao-Ramos, F. Bolás-Fernández, J.J. Torrado, G. Molero, New amphotericin B-gamma cyclodextrin formulation for topical use with synergistic activity against diverse fungal species and *Leishmania* spp, Int. J. Pharm. 473 (2014) 148–157.
[41] R. Espada, J.M. Josa, S. Valdespina, M.A. Dea, M.P. Ballesteros, J.M. Alunda, J. J. Torrado, HPLC assay for determination of amphotericin B in biological samples, Biomed. Chromatogr. 22 (2008) 402–407.
[42] D.R. Serrano, D. Walsh, P. O'Connell, N.A. Mugheirbi, Z.A. Worku, F. Bolas-Fernandez, C. Galiana, M.A. Dea-Ayuela, A.M. Healy, Optimising the in vitro and in vivo performance of oral cocrystal formulations via spray coating, Eur. J. Pharm. Biopharm. 124 (2018) 13–27.
[43] D.R. Serrano, P. O'Connell, K.J. Paluch, D. Walsh, A.M. Healy, Cocrystal habit engineering to improve drug dissolution and alter derived powder properties, J. Pharm. Pharmacol. 68 (2016) 665–677.
[44] D.R. Serrano, T. Persoons, D.M. D'Arcy, C. Galiana, M.A. Dea-Ayuela, A.M. Healy, Modelling and shadowgraph imaging of cocrystal dissolution and assessment of in vitro antimicrobial activity for sulfadimidine/4-aminosalicylic acid cocrystals, Eur. J. Pharm. Sci. 89 (2016) 125–136.
[45] G. Murtaza, H. Ullah, S. Khan, D. Mir, A. Khan, B. Nasir, S. Azhar, M. Abid, Formulation and in vitro dissolution characteristics of sustained-release matrix tablets of tizanidine hydrochloride, Trop. J. Pharm. Res. 14 (2015) 219–225.
[46] K. Wolff, First-order elimination kinetics, in: I.P. Stolerman (Ed.), Encyclopedia of Psychopharmacology, Springer, Berlin Heidelberg, Berlin, Heidelberg, 2010, p. 536.
[47] M.P. Paarakh, P.A. Jose, C.M. Setty, G.V.P. Christoper, Release kinetics – concepts and applications, Int. J. Pharm. Res. Technol. (2019).
[48] S. Yoshioka, V.J. Stella. Stability of Drugs and Dosage Forms, Springer, US, 2002, ISBN 978-0-306-46829-2.
[49] C.o. Europe, Biological tests, in: European Pharmacopoeia 10.0, 2019, pp. 207.
[50] B.C. Evans, C.E. Nelson, S.S. Yu, K.R. Beavers, A.J. Kim, H. Li, H.M. Nelson, T. D. Giorgio, C.L. Duvall, Ex vivo red blood cell hemolysis assay for the evaluation of pH-responsive endosomolytic agents for cytosolic delivery of biomacromolecular drugs, J. Vis. Exp. (2013) e50166.
[51] I. Pineros, K. Slowing, D.R. Serrano, E. de Pablo, M.P. Ballesteros, Analgesic and anti-inflammatory controlled-released injectable microemulsion: pseudo-ternary phase diagrams, in vitro, ex vivo and in vivo evaluation, Eur. J. Pharm. Sci. 101 (2017) 220–227.
[52] Y. Zhang, M. Huo, J. Zhou, S. Xie, PKSolver: An add-in program for pharmacokinetic and pharmacodynamic data analysis in Microsoft Excel, Comput. Methods Programs Biomed. 99 (2010) 306–314.
[53] M. Karimi-Jafari, L. Padrela, G.M. Walker, D.M. Croker, Creating cocrystals: a review of pharmaceutical cocrystal preparation routes and applications, Cryst. Growth Des. 18 (2018) 6370–6387.
[54] N. Park, K. Shin, M. Kang, F. Dowd, B. Johnson, A. Mariotti, Pharmacology and Therapeutics for Dentistry, 2017.
[55] Introduction to tableting by wet granulation, Available from: https://www.dfepharma.com/-/media/documents/technical-documents/technical-papers/introduction-to-tableting-by-wet-granulation.pdf (retrieved on: 1st December 2019).
[56] I. Sukhotnik, J.G. Mogilner, R. Karry, B. Shamian, M. Lurie, N. Kokhanovsky, B. M. Ure, A.G. Coran, Effect of oral glutamine on enterocyte turnover during methotrexate-induced mucositis in rats, Digestion 79 (2009) 5–13.
[57] J. Slavin, Fiber and prebiotics: mechanisms and health benefits, Nutrients 5 (2013) 1417–1435.
[58] S. Yassin, D.J. Goodwin, A. Anderson, J. Sibik, D. Ian Wilson, L.F. Gladden, J. Axel Zeitler, The disintegration process in microcrystalline cellulose based tablets, Part 1: influence of temperature, porosity and superdisintegrants, J. Pharm. Sci. 104 (2015) 3440–3450.
[59] D.R. Serrano, A. Lalatsa, M.A. Dea-Ayuela, P.E. Bilbao-Ramos, N.L. Garrett, J. Moger, J. Guarro, J. Capilla, M.P. Ballesteros, A.G. Schätzlein, F. Bolás, J. J. Torrado, I.F. Uchegbu, Oral particle uptake and organ targeting drives the activity of amphotericin B nanoparticles, Mol. Pharm. 12 (2015) 420–431.
[60] D.D. Bavishi, C.H. Borkhataria, Spring and parachute: How cocrystals enhance solubility, Prog. Cryst. Growth Charact. Mater. 62 (2016) 1–8.
[61] H.R. Guzmán, M. Tawa, Z. Zhang, P. Ratanabanangkoon, P. Shaw, C.R. Gardner, H. Chen, J.P. Moreau, O. Almarsson, J.F. Remenar, Combined use of crystalline salt forms and precipitation inhibitors to improve oral absorption of celecoxib from solid oral formulations, J. Pharm. Sci. 96 (2007) 2686–2702.
[62] T. Ho, R. Aris, On apparent second-order kinetics, AIChE J 33 (1987) 1050–1051.
[63] S. Jun, H. Zhang, J. Bechhoefer, Nucleation and growth in one dimension. I. The generalized Kolmogorov-Johnson-Mehl-Avrami model, Phys. Rev. E Stat. Nonlin. Soft Matter Phys. 71 (2005), 011908.
[64] M.K. Heljak, W. Swieszkowski, K.J. Kurzydlowski, Modeling of the degradation kinetics of biodegradable scaffolds: the effects of the environmental conditions, J. Appl. Polym. Sci. 131 (2014).
[65] Amphotericin B, drug bank information, Available from: https://www.drugbank.ca/drugs/DB00681 (retrieved on: 23rd December 2019).
[66] M.A. Pfaller, D.J. Diekema, D.L. Gibbs, V.A. Newell, E. Nagy, S. Dobiasova, M. Rinaldi, R. Barton, A. Veselov, Candida krusei, a multidrug-resistant opportunistic fungal pathogen: geographic and temporal trends from the ARTEMIS DISK Antifungal Surveillance Program, 2001 to 2005, J. Clin. Microbiol. 46 (2008) 515–521.
[67] D.R. Serrano, L. Hernández, L. Fleire, I. González-Alvarez, A. Montoya, M. P. Ballesteros, M.A. Dea-Ayuela, G. Miró, F. Bolás-Fernández, J.J. Torrado, Hemolytic and pharmacokinetic studies of liposomal and particulate amphotericin B formulations, Int. J. Pharm. 447 (2013) 38–46.
[68] Amphotericin B, data sheet, available from: https://www.sigmaaldrich.com/deepweb/assets/sigmaaldrich/product/documents/134/925/a9528dat.pdf (retrieved on the 15th December 2019).
[69] I. Bekersky, R.M. Fielding, D.E. Dressler, J.W. Lee, D.N. Buell, T.J. Walsh, Plasma protein binding of amphotericin B and pharmacokinetics of bound versus unbound amphotericin B after administration of intravenous liposomal amphotericin B (AmBisome) and amphotericin B deoxycholate, Antimicrob. Agents Chemother. 46 (2002) 834–840.
[70] Itraconazole, data sheet, Available from: https://www.drugbank.ca/drugs/DB01167 (retrieved on: 20th January 2020).
[71] G. Arredondo, E. Suárez, R. Calvo, J.A. Vazquez, J. García-Sanchez, R. Martinez-Jordá, Serum protein binding of itraconazole and fluconazole in patients with diabetes mellitus, J. Antimicrob. Chemother. 43 (1999) 305–307.
[72] Z. Ke, Z. Zhang, H. Wu, X. Jia, Y. Wang, Optimization and evaluation of Oridonin-loaded Soluplus®-Pluronic P105 mixed micelles for oral administration, Int. J. Pharm. 518 (2017) 193–202.
[73] L.A. Tell, A.L. Craigmill, K.V. Clemons, Y. Sun, S.C. Laizure, A. Clifford, J.H. Ina, J. P. Nugent-Deal, L. Woods, D.A. Stevens, Studies on itraconazole delivery and pharmacokinetics in mallard ducks (Anas platyrhynchos), J. Vet. Pharmacol. Ther. 28 (2005) 267–274.
[74] M. Fiore, M. Cascella, S. Bimonte, A.E. Maraolo, I. Gentile, V. Schiavone, M. C. Pace, Liver fungal infections: an overview of the etiology and epidemiology in patients affected or not affected by oncohematologic malignancies, Infect Drug Resist 11 (2018) 177–186.
[75] P. Gershkovich, O. Sivak, E.K. Wasan, A.B. Magil, D. Owen, J.G. Clement, K. M. Wasan, Biodistribution and tissue toxicity of amphotericin B in mice following multiple dose administration of a novel oral lipid-based formulation (iCo-009), J. Antimicrob. Chemother. 65 (2010) 2610–2613.
[76] O. Sivak, P. Gershkovich, M. Lin, E.K. Wasan, J. Zhao, D. Owen, J.G. Clement, K. M. Wasan, Tropically stable novel oral lipid formulation of amphotericin B (iCo-010): biodistribution and toxicity in a mouse model, Lipids Health Dis. 10 (2011) 135.
[77] W.R. Matull, S.P. Pereira, J.W. O'Donohue, Biochemical markers of acute pancreatitis, J. Clin. Pathol. 59 (2006) 340–344.
[78] C.P. Kovesdy, Significance of hypo- and hypernatremia in chronic kidney disease, Nephrol. Dial. Transplant. 27 (2012) 891–898.
[79] E.L. McConnell, A.W. Basit, S. Murdan, Measurements of rat and mouse gastrointestinal pH, fluid and lymphoid tissue, and implications for in-vivo experiments, J. Pharm. Pharmacol. 60 (2010) 63–70.